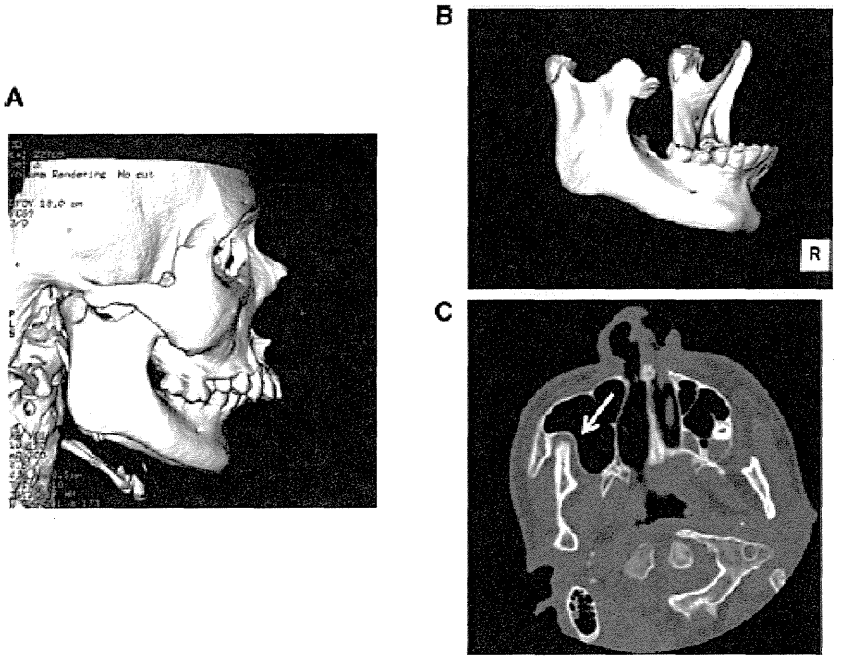

Figure 7. CT made at age 16 years and 3 months. (A) 3-D lateral facial view. (B) Extracted mandible. (C) 2-D view showing HO at the front edge of the right coronoid process. Deformation of bilateral condylar heads, widening of the right coronoid process, and elongation of left coronoid process were observed. HO was found at the anterior edge of the right coronoid process, but it was not fused with upper bones.

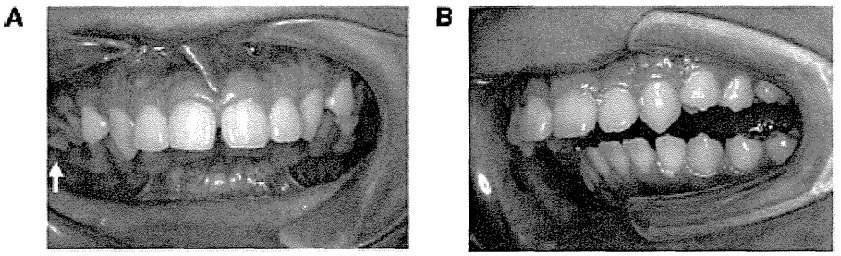

Figure 8. Occlusion at age 19 years and 4 months. (A) In occlusion. Upper right second molar had erupted buccally, showing a scissor bite (arrow). (B) Maximum opening. The maxillary protrusion deteriorated but the amount of mouth opening had slightly improved (6.0 mm).

6.0 mm, respectively. The premolars had erupted normally, but molars had delayed eruption or impaction (Figures 8 and 9). However, the amount of maximum opening slightly improved (6.0 mm). To prevent acute inflammation and subsequent swelling (flare-up) caused by dental caries or periodontal disease, seven molars were extracted under local or general anesthesia. The details of the surgical extraction of the six molars under general anesthesia have been reported previously.[21] The last examination of the patient for this report was at 21 years of age. Bone healing was good at the extraction sites and there was no further deterioration of HO in the facial region. His oral hygiene was excellent and we continue to provide periodic care.

Discussion

Signs or symptoms of FOP are usually not apparent at birth except for the congenital malformation of the great toes; HO often appears within the first decade of life after flare-ups in the soft tissues.[1,2,5,6] When joints are affected by HO, they lose their mobility, and when the vertebral column is affected, it often results in lateral curvature of the column.[1,2,7,12] TMJ and masticatory muscles are also commonly affected, resulting in restricted mouth opening.[5,8-14] The involvement of these tissues occurs relatively late in comparison with other joints, but restricted mouth opening occurs in about half of patients by the age of 20.[7] HO in oral regions appears after trauma or infection, but inadequate dental treatment and acute exacerbation of caries or periodontal disease have also been reported as causative factors.[10,14]

In growing children, HO seems to affect facial growth and occlusion. According to Nussbaum *et al.*,[10] there was a high incidence of mandibular hypoplasia and large overjet in patients with FOP. Renton *et al.*[22] reported flattening of the condylar heads which was found even in patients without restricted mouth opening. However, there are no detailed reports on facial morphology and occlusion, including changes with growth.

Our patient exhibited a skeletal Class II relationship with protrusion of the maxillary alveolar process. The mandible showed normal anteroposterior growth as measured by SNB angle at the age of 8 and 16 years. Flattening of condylar heads was suspected at the first examination and it was clearly seen later in the evaluation of the CT of the head and neck. The restricted mouth opening (5.0 mm) was already recorded at the initial visit. The patient's mother recalled that he had difficulty opening his mouth beginning in infancy. The widening of the right condylar process found at the initial examination was considered to be the cause of the restricted mouth opening. Evaluation of the CT scans made later revealed HO at the front edge of the coronoid process, though the coronoid process was not fused with upper facial

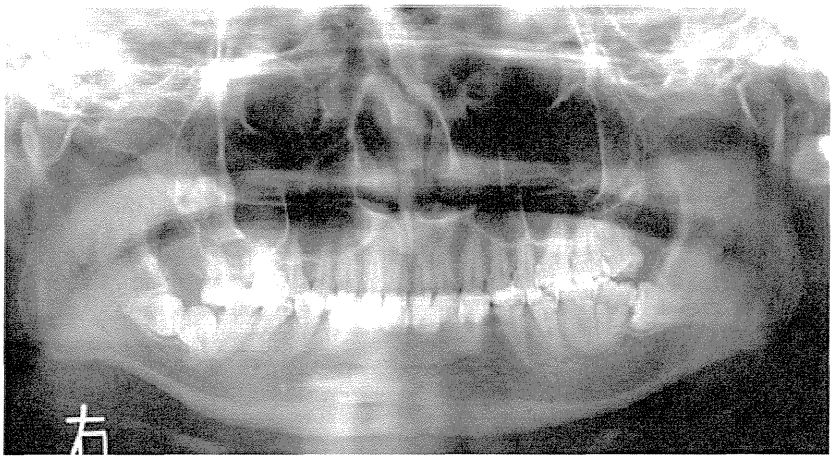

Figure 9. Panoramic radiograph at age 19 years and 5 months. Molars showed abnormal eruption or impaction. Seven molars were later extracted under local or general anesthesia.

bones (Figure 7). This suggested that the restriction was not caused by bone fusion but by mechanical interference of bones on mouth opening as pointed out by Connor and Evans[8] and Nunnelly and Yussen.[9]

Our patient had severe maxillary protrusion with Angle Class II Division 1 occlusion. As Nussbaum *et al.*[10] reported in some of their patients with FOP, this malocclusion seemed to be helpful for cleaning the oral cavity and for eating, as mouth opening was restricted in these patients. If our patient had a normal overjet, the mouth opening would have been smaller. The proclination of maxillary incisors might be caused by forces exerted during masticatory movement.

During follow-up of our patient, the mouth opening did not decrease but rather increased slightly (6.0 mm). Analysis of the cephalogram found that both the maxilla and mandible had greater forward growth than did the anterior cranial base. The ANB angle changed from 9.8° to 12.1° and the overjet changed from 9.5 to 12.0 mm. The forward inclination of both maxillary and mandibular incisors was also increased (Figure 6, Table 1). These changes indicate a probable influence on upper incisor inclination from his hyperactive lower lip as it tried to make an anterior seal during swallowing, and was also influenced by the movement of the tongue on the lower incisors as it thrusts forward to achieve an anterior seal during swallowing. Although the premolars had erupted without problem, the molars were delayed or impacted. This seemed to be due to the lack of eruption space in the posterior region of the mandibular arch. As these molars are more susceptible to dental caries and periodontal disease, seven molars were extracted under local or general anesthesia.[21] After extraction, oral hygiene maintenance became easier than before. At present, a slender toothbrush and an interdental brush are being used for oral cleaning and the patient's oral hygiene is excellent.

The guidelines for dental management of patients with FOP, such as the treatment of caries, tooth extraction, orthodontic treatment, and oral hygiene maintenance, have been proposed by several authors.[19,23] Restricted mouth opening is the main problem, but surgical release of HO has been reported to cause flare-ups and aggravate the HO further.[15] Since it is difficult to carry out dental treatment on these patients, good oral hygiene must be maintained to prevent dental caries and periodontal disease.[19,23,24] Patients should be aware of the problems with oral care methods before the onset of HO and should receive preventive or early interceptive dental treatment. However, even normal opening of the mouth during dental treatment might be traumatic for patients with FOP, and dentists caring for these patients must be aware of this problem.

Maxillary protrusion seems to be common in patients with FOP and orthodontic treatment would be safe.[10] However, the space for cleaning the mouth and eating needs be taken into consideration. If the child shows severe crowding of anterior teeth, orthodontic treatment will be helpful for maintenance of oral hygiene. However, an orthodontic appliance increases the risk of dental caries and gingivitis. Problems with posterior teeth may occur with facial growth similar to our patient, so early and regular dental examination by dentists knowledgeable about FOP is recommended. If abnormal eruption of posterior teeth is found, extraction of the teeth should be considered to prevent dental caries or periodontal disease and to avoid flare-ups and HO.

Conclusion

The patient in this case report had a severely restricted mouth opening caused by HO. He had a Class II facial skeleton and Angle Class II Division 1 occlusion. His maxilla protruded severely but his mandible showed normal anteroposterior development. He also had an abnormally low mandibular plane angle. Orthodontic treatment was not considered because the large overjet enabled him to clean his mouth and to eat. Facial growth was closely monitored over time. As the patient grew, the maxillary protrusion became more prominent and the mandible rotated counterclockwise between the ages of 8 and 16 years. However, the restricted mouth opening did not worsen. The patient's molars had delayed eruption or were impacted, and were extracted under local and general anesthesia. The patient's oral hygiene is currently excellent.

In children with FOP, involvement of the TMJ occurs rather late in comparison with other joints. If FOP is diagnosed at an early age, efforts should be made to

prevent the onset of HO. Oral hygiene maintenance and early preventive or interceptive dental treatment are necessary before the onset of HO. Orthodontic treatment to correct crowding might be helpful for oral hygiene maintenance, but the space for food intake should be taken into consideration if there is restricted mouth opening.

References

1. Kaplan FS, Le Merrer M, Glaser DL, *et al.* Fibrodysplasia ossificans progressiva. *Best Pract Res Clin Rheumatol* 2008;22:191-205.
2. Shore EM, Kaplan FS. Insights from a rare genetic disorder of extra-skeletal bone formation, fibrodysplasia ossificans progressiva (FOP). *Bone* 2008;43:427-33.
3. Shore EM, Xu M, Feldman GJ, *et al.* A recurrent mutation in the BMP type I receptor ACVR1 causes inherited and sporadic fibrodysplasia ossificans progressiva. *Nat Genet* 2006;38:525-7.
4. Kaplan FS, Xu M, Seemann P, *et al.* Classic and atypical fibrodysplasia ossificans progressiva (FOP) phenotypes are caused by mutations in the bone morphogenetic protein (BMP) type I receptor ACVR1. *Hum Mutat* 2009;30:379-90.
5. Rocke DM, Zasloff M, Peeper J, Cohen RB, Kaplan FS. Age- and joint-specific risk of initial heterotopic ossification in patients who have fibrodysplasia ossificans progressiva. *Clin Orthop Relat Res* 1994;301:243-8.
6. Kaplan FS, Xu M, Glaser DL, *et al.* Early diagnosis of fibrodysplasia ossificans progressiva. *Pediatrics* 2008;121:e1295-300.
7. Nakashima Y, Haga N, Kitoh H, *et al.* Deformity of the great toe in fibrodysplasia ossificans progressiva. *J Orthop Sci* 2010;15:804-9.
8. Connor JM, Evans DA. Extra-articular ankylosis in fibrodysplasia ossificans progressiva. *Br J Oral Surg* 1982;20: 117-21.
9. Nunnelly JF, Yussen PS. Computed tomographic findings in patients with limited jaw movement due to myositis ossificans progressiva. *J Oral Maxillofac Surg* 1986;44:818-21.
10. Luchetti W, Cohen RB, Hahn GV, *et al.* Severe restriction in jaw movement after routine injection of local anesthetic in patients who have fibrodysplasia ossificans progressive. *Oral Surg Oral Med Oral Pathol Oral Radiol Endod* 1996;81:21-5.
11. Janoff HB, Zasloff MA, Kaplan FS. Submandibular swelling in patients with fibrodysplasia ossificans progressiva. *Otolaryngol Head Neck Surg* 1996;114: 599-604.
12. Smith R. Fibrodysplasia (myositis) ossificans progressiva. Clinical lessons from a rare disease. *Clin Orthop Relat Res* 1998;346:7-14.
13. van der Meij EH, Becking AG, van der Waal I. Fibrodysplasia ossificans progressiva. An unusual cause of restricted mandibular movement. *Oral Dis* 2006;12:204-7.
14. Sendur OF, Gurer G. Severe limitation in jaw movement in a patient with fibrodysplasia ossificans progressiva: a case report. *Oral Surg Oral Med Oral Pathol Oral Radiol Endod* 2006;102:312-7.
15. Crofford LJ, Brahim JS, Zasloff MA, Marini JC. Failure of surgery and isotretinoin to relieve jaw immobilization in fibrodysplasia ossificans progressiva: report of two cases. *J Oral Maxillofac Surg* 1990;48:204-8.
16. Herford AS, Boyne PJ. Ankylosis of the jaw in a patient with fibrodysplasia ossificans progressiva. *Oral Surg Oral Med Oral Pathol Oral Radiol Endod* 2003;96:680-4.
17. Wadenya R, Fulcher M, Grunwald T, Nussbaum B, Grunwald Z. A description of two surgical and anesthetic management techniques used for a patient with fibrodysplasia ossificans progressiva. *Spec Care Dentist* 2010;30:106-9.
18. Duan Y, Zhang H, Bu R. Intraoral approach technique for treating trismus caused by fibrodysplasia ossificans progressiva. *J Oral Maxillofac Surg* 2010;68:1408-10.
19. Nussbaum BL, Grunwald Z, Kaplan FS. Oral and dental health care and anesthesia for persons with fibrodysplasia ossificans progressiva. *Clin Rev Bone Miner Metab* 2005;3:239-42.
20. Carvalho DR, Pinnola GC, Ferreira DR, *et al.* Mandibular hypoplasia in fibrodysplasia ossificans progressiva causing obstructive sleep apnea with pulmonary hypertension. *Clin Dysmorphol* 2010;19:69-72.
21. Mori Y, Susami T, Haga N, *et al.* Extraction of 6 molars under general anesthesia in patient with fibrodysplasia ossificans progressiva. *J Oral Maxillofac Surg* 2011;69:1905-10.
22. Renton P, Parkin SF, Stamp TC. Abnormal temporomandibular joints in fibrodysplasia ossificans progressiva. *Br J Oral Surg* 1982; 20:31-8.
23. Nussbaum BL, O'Hara I, Kaplan FS. Fibrodysplasia ossificans progressiva: report of a case with guidelines for pediatric dental and anesthetic management. *ASDC J Dent Child* 1996;63:448-50.
24. Young JM, Diecidue RJ, Nussbaum BL. Oral management in a patient with fibrodysplasia ossificans progressiva. *Spec Care Dentist* 2007;27:101-4.
25. Izuka T, Ishikawa F. Normal standards for various cephalometric analyses in Japanese adults. *J Jpn Orthod Soc* 1957;16:4-12.

Gene Therapy (2011) 1 - 5

www.nature.com/gt

SHORT COMMUNICATION

Disease-causing allele-specific silencing against the ALK2 mutants, R206H and G356D, in fibrodysplasia ossificans progressiva

M Takahashi[1], T Katagiri[2], H Furuya[3] and H Hohjoh[1]

Fibrodysplasia ossificans progressiva (FOP) is an autosomal dominant congenital disorder characterized by progressive heterotopic bone formation. Currently, no definitive treatment exists for FOP. The *activin receptor type IA / activin-like kinase 2* (*ACVR1/ALK2*) gene has been identified as the responsible gene for FOP, and disease-associated *ALK2* mutations have been found. Chemical inhibitors to the pathogenic ALK2 receptors are considered possible medical agents for FOP, but their adverse effects on normal ALK2 and other receptors cannot be excluded. Here we describe another treatment strategy for FOP using allele-specific RNA interference (ASP-RNAi), and show modified small interfering RNAs (siRNAs) conferring allele-specific silencing against disease-causing *ALK2* mutants found in FOP, without affecting normal *ALK2* allele. Thus, the siRNAs presented here may become novel therapeutic agents for FOP, and their induced ASP-RNAi may pave the way for the achievement of radical treatment of FOP and/or for the relief of its severe symptoms.

Gene Therapy advance online publication, 1 December 2011; doi:10.1038/gt.2011.193

Keywords: allele-specific RNAi; siRNA; FOP; ALK2; BMP signaling; adverse effects

INTRODUCTION

Fibrodysplasia ossificans progressiva (FOP; MIM#135100) is a rare autosomal dominant disorder characterized by congenital malformation of great toes and progressive heterotopic ossification resulting in skeletal metamorphosis.[1,2] The *activin receptor type IA/activin-like kinase 2* (*ACVR1/ALK2*) gene has been identified as the gene responsible for FOP,[3] and a recurrent mutation, *617G>A(R206H)*, has been found in both familial and sporadic FOP cases of various ethnic groups.[3] In addition, other types of heterozygous *ALK2* mutations have been also detected in patients with atypical FOP, for example, *1067G>A(G356D)*.[1,2,4] The pathogenic, mutant ALK2 receptor appears to be a highly sensitive bone morphogenetic protein (BMP) type I receptor to BMPs and external triggers, resulting in an apparently constitutively active ALK2 receptor, and thereby readily inducing heterotopic bone formation in FOP.[5,6]

Currently, there is no definitive treatment of FOP. Chemical inhibitors against the pathogenic (constitutively active) ALK2 receptors have been developed and could be possible medical agents for FOP. However, they can also inhibit the intracellular signaling of normal ALK2 and other BMP type I receptors (ALK3 and ALK6).[7-9] Thus, adverse effects of the inhibitors may be a major problem to be solved before using them for treatment of FOP.

In this report we show modified small interfering RNAs (siRNAs) conferring allele-specific RNAi against disease-causing *ALK2* mutants found in FOP patients without affecting normal *ALK2* allele, and we propose another treatment strategy for FOP by means of allele-specific silencing.

RESULTS AND DISCUSSION

Specific inhibition of the disease-causing *ALK2* alleles by RNAi could be a potential way for avoidance of adverse effects on normal ALK2 and other receptors,[10] and further for the achievement of treatment of FOP. To achieve such an allele-specific silencing by RNAi (ASP-RNAi), it is vital to design siRNAs capable of discriminating mutant alleles from normal alleles; but it is quite difficult. Our previously established assay system with two reporter alleles encoding the *Photinus* and *Renilla luciferase* genes carrying mutant and wild-type allelic sequences in their 3′-untranslated regions may solve the problem and allow for determination of such siRNAs.[11-14] Briefly, test siRNAs are co-transfected with the mutant and wild-type reporter alleles and the *β-galactosidase* gene as a control into HeLa cells, and 24 h after transfection, dual-luciferase and β-galactosidase assays are carried out. Note that the transfected cells are heterozygous with the mutant and wild-type reporter alleles; thus, the effects of the test siRNAs on suppression of both the target mutant and non-target wild-type reporter alleles can be simultaneously examined. Using the assay system, we attempted to design competent siRNAs conferring allele-specific silencing against two distinct *ALK2* mutants found in FOP: one is *ALK2_617G>A(R206H)* and the other is *ALK2_1067G>A(G356D)*, which is a rare mutation found in a variant FOP case.[4]

The mutant *ALK2* reporter alleles carrying the *ALK2_617G>A(R206H)* and *ALK2_1067G>A(G356D)* mutations and their corresponding normal (wild-type) reporter alleles were constructed (Supplementary Figure S1). SiRNAs targeting the mutant *ALK2* were chemically synthesized (Supplementary Tables S1 and S2) and subjected to screening (assessment) by the assay system with the reporter alleles. The first screening of the siRNAs perfectly matched the mutant sequences, resulted in a negative consequence except for the siG356D_A9 siRNA (Supplementary Figure S2); siG356D_A9 appeared to induce allele-specific silencing in a moderate level.

[1]Department of Molecular Pharmacology, National Institute of Neuroscience, NCNP, Kodaira, Tokyo, Japan; [2]Division of Pathophysiology, Research Center for Genomic Medicine, Saitama Medical University, Hidaka-shi, Saitama, Japan and [3]Department of Neurology, Neuro-Muscular Center, National Omuta Hospital, Fukuoka, Japan. Correspondence: Dr H Hohjoh, Department of Molecular Pharmacology, National Institute of Neuroscience, NCNP, 4-1-1 Ogawahigashi, Kodaira, Tokyo 187-8502, Japan.
E-mail: hohjohh@ncnp.go.jp
Received 13 June 2011; revised 6 October 2011; accepted 10 October 2011

Modification of siRNAs such as introduction of mismatched base(s) into siRNAs often provides improvement in allele discrimination of the modified siRNAs,[12,14] thereby enhancing ASP-RNAi. It is known that nucleotide mismatches between siRNAs and their target RNAs can influence RNAi activity; however, critical nucleotide position(s) and kinds of nucleotide mismatches for conferring allele discrimination are still unpredictable: this may be because different siRNAs have different features depending upon their different nucleotide sequences. Therefore, modified siRNAs must be examined one by one for their allele discrimination abilities, and our assay system seems to be useful for such an assessment.

We designed various mismatched siRNAs (Supplementary Tables S1 and S2) and tested them by the assay system. From a series of assessment (Supplementary Figures S3 and S4), the siR206H_A9(C14) and siG356D_A10(A13) modified siRNAs showed a marked improvement of their allele-specific silencing against the *ALK2_617G>A(R206H)* and *ALK2_1067G>A(G356D)* mutant reporter alleles, respectively (Figures 1a and b and Figures 1c and d, respectively). The 50% inhibitory concentrations (IC_{50} values) of the siRNAs further verified their remarkable allele discrimination (Figures 1b and d): the IC_{50} values of siR206H_A9(C14) and siG356D_A10(A13) against their target mutant alleles were 0.61 and 0.27 nM, respectively, whereas the IC_{50} values against the normal alleles were >20 nM, suggesting that the siR206H_A9(C14)- and siG356D_A10(A13)-modified siRNAs have the potential for suppressing the mutant *ALK2* alleles carrying *617G>A(R206H)* and *1067G>A(G356D)*, respectively, without affecting the normal *ALK2* allele.

We examined knockdown potencies of the siR206H_A9(C14)- and siG356D_A10(A13)-modified siRNAs against *bona fide* mutant ALK2 receptors by introduction of the siRNAs and expression plasmid carrying the mutant (*ALK_R206H* or *ALK_G356D*) or normal *ALK2* cDNA into C2C12 myoblasts. As shown in Figures 2a and b, the modified siRNAs successfully inhibited the expression of their target mutant receptors without inhibiting the expression of the normal ALK2 receptor.

When the modified siRNAs and expression plasmids were introduced into cells together with the BMP-specific luciferase reporter gene (IdWT4F-luc) whose expression is induced by mutant ALK2 receptors,[15] the siRNAs significantly and specifically inhibited the IdWT4F-luc activities induced by their target mutant ALK2 receptors; however, they did not induce any suppression to the activities involving normal or non-target mutant ALK2 receptors (Figure 2c). In addition, it should be noted that the siRNAs triggered no inhibition of the IdWT4F-luc activity induced by ALK2_Q207D that was another mutant ALK2 receptor studied as a control. Taken together, these findings suggest that the siR206H_A9(C14)- and siG356D_A10(A13)-modified siRNAs can induce a specific inhibition against their target mutant ALK2 receptors without suppressing normal ALK2 receptor.

Next we examined the effects of the modified siRNAs on disease-causing allele specific silencing against endogenous ALK2 mutants in lymphoblastoid cells established from FOP patients carrying the *ALK2_R206H* or *ALK2_G356D* allele: the lymphoblastoid cell might be a useful model for examining the BMP pathway in FOP patients.[16] Introduction of the IdWT4F-luc reporter gene into the lymphoblastoid cells revealed that: (1) the IdWT4F-luc activity was significantly upregulated in FOP patient cells expressing ALK2_R206H, and (2) the level of the IdWT4F-luc activity in another patient cells expressing ALK2_G356D was as low as that in healthy individual cells (N001; Figure 3a). These results were consistent with our previous finding that ALK2_G356D had less activity than ALK2_R206H.[17] On the basis of the data, we introduced the siR206H_A9(C14) siRNA together with the IdWT4F-luc reporter gene into patient cells expressing ALK2_R206H. The result demonstrated significant reduction of the IdWT4F-luc activity by siR206H_A9(C14) (Figure 3b); and marked decrease in the *ALK2_R206H* transcript was consistently detected, whereas the level of the normal *ALK2* transcript, by contrast, remained unchanged (Figure 3c). Therefore, these findings strongly suggest that ASP-RNAi by our modified siRNAs can produce a specific inhibition against the pathogenic, constitutively active BMP signaling caused by mutant ALK2 receptors in FOP, and also confers few adverse effects on normal ALK2 receptor.

In conclusion, although chemical inhibitors to the BMP type I receptors could be possible medicinal agents for FOP,[5,8] they further affect normal ALK2 receptor[7] and other BMP type I receptors,[9] as well as pathogenic (mutant) ALK2 receptors. Thus, the risk of adverse effects of the inhibitors cannot be excluded at present, and such problems remain to be solved. In this study, we showed modified (mismatched) siRNAs conferring ASP-RNAi against two distinct disease-causing *ALK2* alleles without affecting normal *ALK2* allele. Therefore, the siRNAs may be capable of becoming novel medical agents for FOP, and disease-causing allele specific silencing by ASP-RNAi may provide patients with a safe treatment with few adverse effects.

Disease-causing *ALK2* mutations other than *ALK2_617G>A(R206H)* and *ALK2_1067G>A(G356D)* may also be targets for ASP-RNAi, and our assessment system may allow for designing competent siRNAs conferring disease-causing allele specific silencing targeting such *ALK2* mutants. Therefore, diagnoses including *ALK2* mutation analysis by PCR-direct sequencing or TaqMan probes are vital for selection of appropriate treatment of FOP.

To achieve *in vivo* ASP-RNAi, drug delivery system for siRNAs is also vital; and drug delivery system using stealth liposomes[18] and atelocollagen,[19,20] which appears to reduce recognition by the reticuloendothelial system, may be promising. To establish a safe and stable transport of siRNAs *in vivo* for RNAi therapy, more extensive studies remain to be carried out in the future.

Finally, RNAi therapy as another medical treatment strategy might pave a new path for the achievement of curative treatment

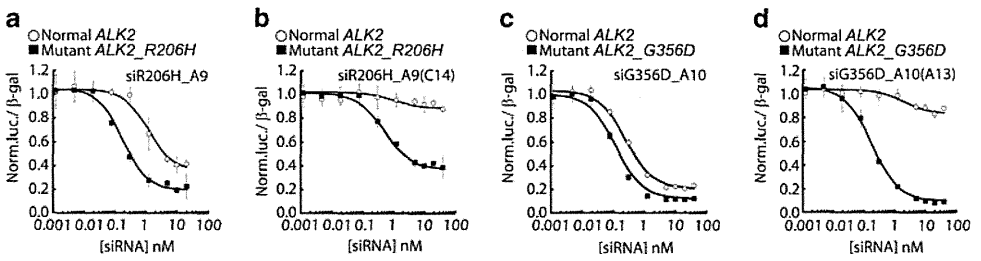

Figure 1. Allele-specific silencing against mutant *ALK2* reporter alleles. The effects of conventional and modified siRNAs on allele-specific silencing were examined by IC_{50} analysis: siR206H_A9 (**a**) and siG356D_A10 (**c**) are conventional siRNAs, and siR206H_A9(C14) (**b**) and siG356D_A10(A13) (**d**) are modified (mismatched) siRNAs. Data of mutant and normal reporter alleles are indicated by the solid squares and open circles, respectively. Note that the modified siRNAs markedly improved allele discrimination or allele-specific silencing (**b**, **d**). Data shown are average of four independent determinations. Error bars represent s.d.'s.

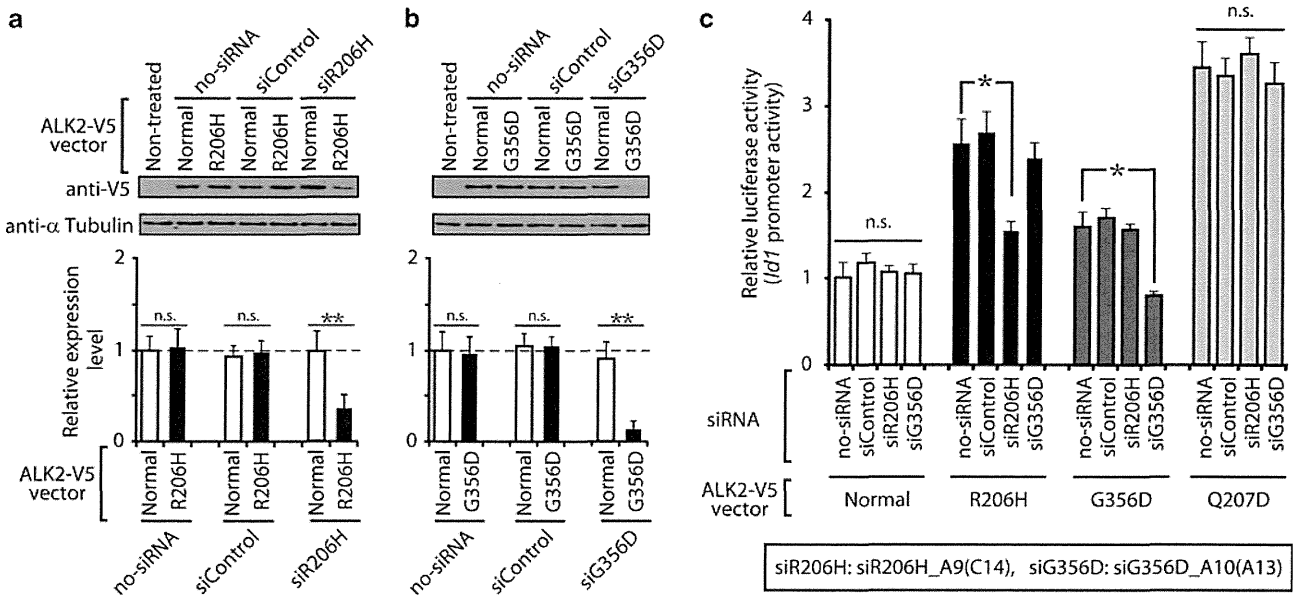

Figure 2. Specific inhibition of mutant ALK2 receptors by ASP-RNAi. The siR206H_A9(C14) (siR206H) and siG356D_A10(A13) (siG356D) modified siRNAs and non-silencing siRNA control (siControl) were co-transfected with expression plasmid encoding the V5-tagged *ALK_R206H* (**a**), *ALK_G356D* (**b**) or normal *ALK2* cDNA into C2C12 myoblasts. After 2-day incubation, the level of ALK2 was examined by western blotting with anti-V5 antibody. Non-treated cells were also examined as a control. The relative expression levels are indicated in the graphs. Data shown are average of four independent measurements with s.d.'s. $^{**}P<0.01$, between indicated pairs. (**c**) Specific inhibition of BMP signaling involving mutant ALK2 receptors. The pIdWT4F-luc plasmid encoding BMP-specific luciferase reporter gene and the phRL-TK plasmid carrying the *Renilla luciferase* gene as a control were co-transfected with indicated siRNAs and ALK2 expression plasmids (Normal, R206H, G356D and Q207D) into C2C12 cells. The *Photinus luciferase* activity of IdWT4F-luc was normalized to the *Renilla* luciferase activity as a control, and the data were further normalized to the data obtained from the control cells, in which the normal ALK2 was expressed in the absence of siRNA (no siRNA in Normal). Data shown are average of four independent determinations with s.d.'s. $^{*}P<0.05$, between indicated pairs. n.s., no statistical significance.

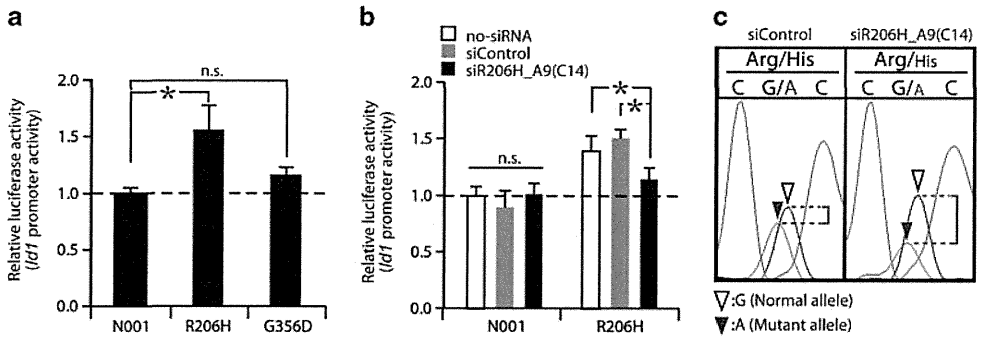

Figure 3. Suppression of pathogenic BMP signaling caused by endogenous mutant ALK2. (**a**) Constitutively active BMP signaling in FOP patient cells. Lymphoblastoid cells were established from FOP patients carrying the *ALK2_R206H* (R206H) or *ALK2_G356D* (G356D) mutation and from a healthy individual (N001). The cells were subjected to transfection with the pIdWT4F-luc and phRL-TK plasmids, and the expression levels of the luciferase reporters were examined as in Figure 2c. Data shown are average of three independent determinations with s.d.'s. $^{*}P<0.05$, between indicated pairs. (**b**) Suppression of pathogenic, constitutively active BMP signaling. The siR206H_A9(14C) or siControl siRNAs were transfected with the pIdWT4F-luc and phRL-TK plasmids into patient cells expressing the AKL2_R206H (R206H) receptor and healthy individual cells (N001). The expression levels of the luciferases were examined as in Figure 2c. Data shown are average of three independent determinations with s.d.'s. $^{*}P<0.05$, between indicated pairs. (**c**) Direct sequencing. Total RNAs were extracted from patient cells expressing *ALK2_R206H* in the presence of siR206H_A9(14C) or siControl, and subjected to RT-PCR followed by direct sequencing. The Arg(CGC) and His(CAC) codons at amino-acid position 206 in the normal and mutant alleles, respectively, are shown. The peaks of the normal guanine and mutant adenine bases are indicated by open and solid arrowheads, respectively; and the difference between the peaks is indicated by a bar in red. n.s., no statistical significance.

of FOP and/or for relief of its severe symptoms; and our current study may further shed some light on the availability of ASP-RNAi as a disease-causing allele specific silencing tool, for medical treatment of intractable diseases caused by dominant-positive alleles, such as FOP.

MATERIALS AND METHODS

Cell culture

HeLa and C2C12 cells were grown at 37 °C in Dulbecco's modified Eagle's medium (Wako, chuo-ku, Osaka, Japan) supplemented with 10% and 15% fetal bovine serum (Invitrogen, Carlsbad, CA, USA), respectively, 100 U ml^{-1}

penicillin and 100 μg ml^{-1} streptomycin (Wako) in a 5% CO_2 humidified chamber. Epstein-Barr virus-transformed human lymphoblastoid cell lines were cultured at 37 °C in RPMI1640 medium (Sigma-Aldrich, St Louis, MO, USA) supplemented with 10% fetal bovine serum (Japan Bio Serum, Fukuyama, Hiroshima, Japan), 110 mg l^{-1} sodium pyruvate (Wako), 4500 mg l^{-1} D-glucose (Wako), 100 U ml^{-1} penicillin and 100 μg ml^{-1} streptomycin (GIBCO, Carlsbad, CA, USA) in a 5% CO_2 humidified chamber. The Ethics Committees of the National Center of Neurology and Psychiatry, National Omuta Hospital and Saitama Medical University approved the study with Epstein-Barr virus-transformed human lymphoblastoid cell lines derived from FOP patients.

DNA and RNA oligonucleotides

DNA oligonucleotides and siRNAs used in this study were obtained from Sigma-Aldrich. The sequences of the synthesized oligonucleotides are indicated in Supplementary Tables S1, S2 and S3.

Construction of mutant and wild-type reporter alleles

Mutant and wild-type reporter alleles were constructed as described previously.[11,13] Briefly, phRL-TK (Promega, Fitchburg, WI, USA) and pGL3-TK plasmids encoding the *Renilla* and *Photinus luciferase* genes, respectively, were digested with *Xba*I and *Not*I, and subjected to ligation with synthetic oligonucleotide duplexes corresponding to the *ALK2* normal, *R206H (617G>A)* and *G356D (1067G>A)* mutant alleles (Supplementary Figure S1). The oligonucleotide sequences for the construction of the reporter alleles are indicated in Supplementary Table S3.

Assessment of siRNAs

Transfection of designed siRNAs together with the constructed reporter alleles, and luciferase and β-galactosidase assays were carried out as described previously.[11,13] Briefly, the day before transfection, HeLa cells were trypsinized, diluted with fresh medium without antibiotics and seeded into 96-well culture plates (~1 × 10^5 cells per cm^2). The pGL3-TK-backbone reporter allele plasmid (60 ng), phRL-TK-backbone reporter allele plasmid (10 ng) and pSV-β-galactosidase control plasmid (20 ng; Promega) were co-transfected with designed siRNA (20 nM , final concentration) into each well using Lipofectamine 2000 transfection reagent (Invitrogen) according to the manufacturer's instructions. Twenty-four hours after transfection, cell lysate was prepared and the expression levels of the *Photinus* and *Renilla* luciferases and β-galactosidase were examined by Dual-Luciferase reporter assay system (Promega) and Beta-Glo assay system (Promega), respectively. The luminescent signal was measured by a Fusion Universal Microplate Analyzer (PerkinElmer, Waltham, MA, USA). The levels of mutant and wild-type luciferase reporter allele activities were normalized to the level of β-galactosidase activity as a control, and the resultant ratios of the mutant and wild-type reporter allele activities in the presence of the test siRNAs were further normalized to the control ratios obtained in the presence of a non-silencing siRNA (siControl).

For examination of dose-dependent inhibition of siRNA (IC_{50} of siRNA), the plasmids described above were co-transfected with an increasing amount of each siRNA (0, 0.001, 0.005, 0.02, 0.08, 0.32, 1.25, 5, 10 and 20 nM (final concentration)) into each well using Lipofectamine 2000 transfection reagent. Twenty-four hours after transfection, the expression of luciferase and β-galactosidase was examined as described above. The data were fitted to the Hill equation (Hill coefficient; $n = 1$) and IC_{50} values were determined.

Examination of active BMP signaling pathway using pIdWT4F-luc plasmid

The IdWT4F-luc reporter plasmid carrying the *Photinus luciferase* gene driven by the *Id1* promoter, which is activated by BMP signaling, was used,[15] and the basic assay system for the BMP pathway using C2C12 myoblast cells followed the previous study.[17] The day before transfection, C2C12 myoblast cells were trypsinized and seeded into 24-well culture plates (~1 × 10^5 cells per cm^2) in culture medium without antibiotics. Co-transfection of the IdWT4F-luc plasmid (100 ng per well) together with normal- or mutant-type *ALK2-V5* expression plasmid (200 ng per well),[15,17] designed siRNA duplexes (20 nM, final concentration) and phRL-TK plasmid (50 ng per well) as a control was carried out using Lipofectamine 2000 transfection reagent. Two days after transfection, cell lysate was prepared and the expression levels of luciferase reporter genes were examined by Dual-Luciferase reporter assay system (Promega) according to the manufacturer's instructions. The luminescent signals were measured by a Fusion Universal Microplate Analyzer (PerkinElmer).

Western blot analysis

Equal amount of proteins was separated by SDS-PAGE with 10% polyacrylamide gels (10% T, 3.3% C), and electrophoretically blotted onto PVDF membranes (Millipore, Billerica, MA, USA). The membranes were blocked in blocking solution (5% skim milk in phosphate-buffered saline containing 0.05% Tween-20), and incubated with 1/5000 diluted anti-V5 antibody (Invitrogen) or 1/20 000 diluted mouse anti-α tubulin monoclonal antibody (Sigma-Aldrich) followed by washing in phosphate-buffered saline containing 0.05% Tween-20. After washing, further incubation with 1/5000 diluted horseradish peroxidase-conjugated anti-mouse IgG (Sigma-Aldrich) was carried out. Antigen-antibody complexes were visualized using Immobilon Western Chemiluminescent HRP Substrate (Millipore). The signal intensities of the visualized bands were measured by a Scion Image (Scion Corporation, Frederick, MD, USA). The data of the ALK2-V5 band were normalized to the intensity of the α-tubulin band, and further normalized to those obtained from naïve (non-treated) cells.

Electroporation

Introduction of the pIdWT4F-luc and phRL-TK plasmids together with siRNA into lymphoblastoid cells was carried out by means of the Nucleofector system (Amaxa, Basel, Switzerland) according to the manufacturer's instructions. Briefly, the cells (1 × 10^6 cells per transfection) were suspended in 100 μl of electroporation buffer (Cell Line Nucleofector Solution V; Amaxa) containing 5 μM of siRNA, 300 ng of pIdWT4F-luc and 200 ng of phRL-TK plasmid. The transfection mixtures were subjected to electroporation with the U-005 pulsing program. After electroporation, the cells were immediately transferred into six-well culture plates containing pre-warmed culture medium and were incubated for 2 days.

Direct sequencing

Total RNAs were extracted from lymphoblastoid cells, which were cultured for 2 days after electroporation, and subjected to cDNA synthesis with Oligo(dT)$_{15}$ primers (Promega) and a Superscript III reverse transcriptase (Invitrogen) according to the manufacturer's instructions. PCR was carried out with the cDNA as a template and a primer set for amplification of a region containing the *ALK2_R206H(617G>A)* mutation using the GeneAmp PCR system 3700 (Applied Biosystems, Carlsbad, CA, USA). The thermal cycling profiles were as follows: heat denaturation at 94 °C for 1 min, 30 cycles of amplification including denaturation at 98 °C for 10 s, and annealing and extension at 68 °C for 1 min. The resultant PCR products were purified by a PCR and Gel purification kit (BEX, Itabashi-ku, Tokyo, Japan) according to the manufacturer's instructions, and subjected to direct sequencing by means of the ABI 3730 *xl* DNA Analyzer (Applied Biosystems). The sequences of the PCR and direct-sequencing primers were as follows: *ALK2(R206H)* primer set:

5′-CACCACCAATGTTGGAGACAGC-3′
5′-CTGAACCATGACTTCTCATCACG-3′.

Statistical analysis

To examine the effect of disease-causing allele-specific RNAi knockdown, all statistical analysis was carried out using analysis of variance. When significant difference was shown by analysis of variance, Tukey's *post hoc* test was further carried out. The level of statistical significance was set at 0.05.

CONFLICT OF INTEREST

The authors declare no conflict of interest.

ACKNOWLEDGEMENTS

This work was supported by research grants from the Ministry of Health, Labour and Welfare of Japan and from the National Hospital Organization, and also by Grants-in-Aid for Scientific Research from the Japan Society for the Promotion of Science and by Grant-in-Aid for Young Scientists (Start-up).

REFERENCES

1 Shore EM, Kaplan FS. Role of altered signal transduction in heterotopic ossification and fibrodysplasia ossificans progressiva. *Curr Osteoporos Rep* 2011; **9**: 83-88.
2 Katagiri T. Heterotopic bone formation induced by bone morphogenesis protein signaling: fibrodysplasia ossificans progressiva. *J Oral Biosci* 2010; **52**: 33-41.
3 Shore EM, Xu M, Feldman GJ, Fenstermacher DA, Cho TJ, Choi IH *et al.* A recurrent mutation in the BMP type I receptor ACVR1 causes inherited and sporadic fibrodysplasia ossificans progressiva. *Nat Genet* 2006; **38**: 525-527.
4 Furuya H, Ikezoe K, Wang L, Ohyagi Y, Motomura K, Fujii N *et al.* A unique case of fibrodysplasia ossificans progressiva with an ACVR1 mutation, G356D, other than the common mutation (R206H). *Am J Med Genet A* 2008; **146A**: 459-463.
5 Fukuda T, Kohda M, Kanomata K, Nojima J, Nakamura A, Kamizono J *et al.* Constitutively activated ALK2 and increased SMAD1/5 cooperatively induce bone morphogenetic protein signaling in fibrodysplasia ossificans progressiva. *J Biol Chem* 2009; **284**: 7149-7156.
6 Shen Q, Little SC, Xu M, Haupt J, Ast C, Katagiri T *et al.* The fibrodysplasia ossificans progressiva R206H ACVR1 mutation activates BMP-independent chondrogenesis and zebrafish embryo ventralization. *J Clin Invest* 2009; **119**: 3462-3472.
7 Hao J, Ho JN, Lewis JA, Karim KA, Daniels RN, Gentry PR *et al. In vivo* structure-activity relationship study of dorsomorphin analogues identifies selective VEGF and BMP inhibitors. *ACS Chem Biol* 2010; **5**: 245-253.
8 Yu PB, Deng DY, Lai CS, Hong CC, Cuny GD, Bouxsein ML *et al.* BMP type I receptor inhibition reduces heterotopic [corrected] ossification. *Nat Med* 2008; **14**: 1363-1369.
9 Yu PB, Hong CC, Sachidanandan C, Babitt JL, Deng DY, Hoyng SA *et al.* Dorsomorphin inhibits BMP signals required for embryogenesis and iron metabolism. *Nat Chem Biol* 2008; **4**: 33-41.
10 Kaplan J, Kaplan F, Shore EM. Development of allele-specific RNAi as a therapeutic strategy for fibrodysplasia ossificans progressiva. *J Bone Miner Res* 2009 (Supplement-1) (http://www.asbmr.org/Meetings/AnnualMeeting/AbstractDetail.aspx?aid=59e0e08f-6568-4b1b-80d5-fcc93765f2a5).
11 Hohjoh H. Allele-specific silencing by RNA interference. *Methods Mol Biol* 2010; **623**: 67-79.
12 Ohnishi Y, Tamura Y, Yoshida M, Tokunaga K, Hohjoh H. Enhancement of allele discrimination by introduction of nucleotide mismatches into siRNA in allele-specific gene silencing by RNAi. *PLoS One* 2008; **3**: e2248.
13 Ohnishi Y, Tokunaga K, Kaneko K, Hohjoh H. Assessment of allele-specific gene silencing by RNA interference with mutant and wild-type reporter alleles. *J RNAi Gene Silencing* 2006; **2**: 154-160.
14 Takahashi M, Watanabe S, Murata M, Furuya H, Kanazawa I, Wada K *et al.* Tailor-made RNAi knockdown against triplet repeat disease-causing alleles. *Proc Natl Acad Sci USA* 2010; **107**: 21731-21736.
15 Katagiri T, Imada M, Yanai T, Suda T, Takahashi N, Kamijo R. Identification of a BMP-responsive element in Id1, the gene for inhibition of myogenesis. *Genes Cells* 2002; **7**: 949-960.
16 Kaplan FS, Fiori J, LS DLP, Ahn J, Billings PC, Shore EM. Dysregulation of the BMP-4 signaling pathway in fibrodysplasia ossificans progressiva. *Ann N Y Acad Sci* 2006; **1068**: 54-65.
17 Fukuda T, Kanomata K, Nojima J, Kokabu S, Akita M, Ikebuchi K *et al.* A unique mutation of ALK2, G356D, found in a patient with fibrodysplasia ossificans progressiva is a moderately activated BMP type I receptor. *Biochem Biophys Res Commun* 2008; **377**: 905-909.
18 Podesta JE, Kostarelos K. Chapter 17 - Engineering cationic liposome siRNA complexes for *in vitro* and *in vivo* delivery. *Methods Enzymol* 2009; **464**: 343-354.
19 Hanai K, Takeshita F, Honma K, Nagahara S, Maeda M, Minakuchi Y *et al.* Atelocollagen-mediated systemic DDS for nucleic acid medicines. *Ann N Y Acad Sci* 2006; **1082**: 9-17.
20 Ochiya T, Takahama Y, Nagahara S, Sumita Y, Hisada A, Itoh H *et al.* New delivery system for plasmid DNA *in vivo* using atelocollagen as a carrier material: the Minipellet. *Nat Med* 1999; **5**: 707-710.

Supplementary Information accompanies the paper on Gene Therapy website (http://www.nature.com/gt)

Acta Pharmaceutica Sinica B 2012;2(1):23–27

Institute of Materia Medica, Chinese Academy of Medical Sciences
Chinese Pharmaceutical Association

Acta Pharmaceutica Sinica B

www.elsevier.com/locate/apsb
www.sciencedirect.com

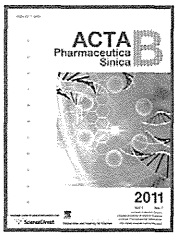

ORIGINAL ARTICLE

Fungal pyrrolidine-containing metabolites inhibit alkaline phosphatase activity in bone morphogenetic protein-stimulated myoblastoma cells

Takashi Fukuda[a], Ryuji Uchida[a], Hiroyo Inoue[a], Satoshi Ohte[b], Hiroyuki Yamazaki[a], Daisuke Matsuda[a], Takenobu Katagiri[b], Hiroshi Tomoda[a,*]

[a]*Graduate School of Pharmaceutical Sciences, Kitasato University, Tokyo, Japan*
[b]*Research Center for Genomic Medicine, Saitama Medical University, Saitama, Japan*

Received 21 October 2011; revised 10 November 2011; accepted 12 December 2011

KEY WORDS

Lucilactaenes;
Fungal metabolites;
C2C12 myoblasts;
Fibrodysplasia ossificans progressiva

Abstract Fibrodysplasia ossificans progressiva (FOP) is a rare autosomal dominant congenital disorder characterized by progressive heterotopic ossification in muscle tissues. A constitutively activated mutation of a bone morphogenetic protein (BMP) receptor, ALK2, has been identified in patients with FOP. We report here that four structurally related compounds, lucilactaene, hydroxylucilactaene, NG-391 and NG-393, produced by fungal strain *Fusarium* sp. B88, inhibit BMP signaling *in vitro*. Alkaline phosphatase activity, a marker enzyme of osteoblastic differentiation, was decreased in C2C12 myoblasts stably expressing mutant ALK2 by treatment with those compounds with IC_{50} values of 5.7, 6.8, 6.9 and 6.1 μM, respectively. Furthermore, NG-391 and NG-393 inhibited BMP-specific luciferase reporter activity, which is directly regulated by transcription factor Smads, with IC_{50} values of 1.4 and 2.1 μM, respectively. These findings suggest that these fungal metabolites may provide a new direction in the development of FOP therapeutics.

*Corresponding author. Tel.: +81 3 5791 6241; fax: +81 3 3444 6197.
E-mail address: tomodah@pharm.kitasato-u.ac.jp (Hiroshi Tomoda).

Peer review under responsibility of Institute of Materia Medica, Chinese Academy of Medical Sciences and Chinese Pharmaceutical Association.
doi:10.1016/j.apsb.2011.12.011

Production and hosting by Elsevier

1. Introduction

Bone is a connective tissue that guarantees the protection and support of organ function. Contrary to the common view, bone is a dynamic tissue that constantly undergoes turnover in order to maintain stability and remodeling. Bone remodeling is a process coupled with bone resorption and bone formation that determines bone structure and quality during adult life. Osteoblasts, bone-forming cells, are derived from the embryonic mesoderm. During the early stages of osteoblast differentiation, several molecules such as bone morphogenetic proteins (BMPs), transforming growth factor-βs (TGF-βs), leukemia inhibitor factor (LIF), fibroblast growth factors (FGFs) and platelet-derived growth factors (PDGFs), drive the differentiation of stem cells to inducible osteoprogenitors (stromal mesenchymal stem cells) and then to determined osteoprogenitors[1]. Among these molecules, BMPs are reported as unique factors, which can induce ectopic bone formation in muscle[2].

The BMP signaling pathway is one of the most highly conserved signaling pathways among the bone remodeling systems[3,4]. The BMP signal starts with binding to heterotetrameric transmembrane complexes of type I and type II BMP receptors. Four type I receptors, ALK1, ALK2, ALK3/BMPR-IA and ALK6/BMPR-IB, and three type II receptors, BMPR-II, ActR-II and ActR-IIB, have been reported[5]. Following ligand binding, serines and threonines in the glycine/serine (GS) domain of type I receptor are phosphorylated by the constitutively activated type II receptor. Thus, the BMP type I receptor is activated by the phosphorylation event, which transmits downstream to BMP pathway-specific Smad1/5/8 and p38 MAPK[6]. Furthermore, phosphorylated Smad1/5/8 forms complexes with Smad4, and they move to the nucleus and work as transcription factors to express early responsive genes such as Id1 (an inhibitory protein for myogenesis). Smads bind to a GC-rich BMP responsive element (BRE) in the early responsive genes[6]. The cells activated via BMP signaling differentiate to osteoblastic cells, which express typical differentiation markers such as alkaline phosphatase (ALP), osteocalcin and osteopontin.

Fibrodysplasia ossificans progressiva (FOP) is a congenital disorder of progressive and widespread postnatal ossification of soft tissues[7]. Ectopic bone formation in FOP occurs through an endochondral pathway in which cartilage is formed initially at the site and is subsequently replaced by bone[8,9]. FOP results in severe debilitation and reduces the life span due to joint fusion and restrictive lung disease with thoracic involvement. The median age of survival is approximately 41 years[10]. Surgical attempts to operatively remove heterotopic bone have commonly led to episodes of explosive and painful new bone growth called "flare-ups"[11]. Shore et al.[12] found a recurrent heterozygous mutation, c.617G→A, in the *ACVR1/ALK2* gene in both familial and sporadic patients with FOP that causes an amino acid substitution of Arg to His at codon 206 (R206H) of ALK2. Since this mutation has been shown to constitutively activate ALK2, specific inhibitors of ALK2 could offer therapeutic benefit for FOP. Consequently, the quest for novel pharmacological agents that target specific steps of FOP has significantly intensified. As a result, synthetic dorsomorphin[13,14], originally discovered as an AMP kinase inhibitor, was found to selectively inhibit BMP signaling induced by type I receptors such as ALK2, ALK3 and ALK6[13]. Cuny et al.[15] improved dorsomorphin to successfully obtain more potent derivative LDN-193189, which prevented ectopic bone formation in mice carrying an active mutant ALK2 and attenuated lesions in the remainder[16]. C2C12 myoblasts, derived from murine thigh muscle, inhibit myogenesis and express osteoblastic phenotypes by treatment with BMPs or over-expression of constitutively activated BMP type I receptors[6]. C2C12 cells have been widely used for studies of osteoblast differentiation induced by BMP signaling *in vitro*[17–19].

In this study, we screened for potent inhibitors of osteoblastic differentiation induced by BMP signaling using a stable ALK2(R206H)-expressing C2C12 cell line (abbreviated as C2C12(R206H) cells), which exhibited ALP activity more quickly and more strongly than original C2C12 cell line, to develop FOP chemotherapy[20]. After testing the natural product library (217 compounds) and the actinomycetal and fungal culture broths (9831 samples) in this screening, we found four structurally related fungal metabolites, lucilactaene[21], hydroxylucilactaene[22], NG compounds (NG-391 and NG-393)[23,24], from the culture broth of *Fusarium* sp. B88. Moreover, NG-391 and NG-393 inhibited a BMP-specific luciferase reporter activity, which is directly regulated by transcription factor Smads. These findings suggest that these fungal metabolites may provide a new direction in the development of FOP therapeutics.

2. Materials and methods

2.1. Materials

Fusarium sp. B88 was isolated from the body of a grasshopper collected in 2006 on Ishigakijima where is a small southern island belonging to Okinawa in Japan. This fungus was incubated in BYK-1 broth (25 g RISO VIALONE NANO RICE (Japan Europe Trading Co., Ltd., Tokyo, Japan) and 0.6 g Difco™ Potato Dextrose Broth (Becton, Dickinson Company, France) in 25 mL H_2O) at 27 °C for 14 day under static conditions. The culture broth (1 kg) was extracted with acetone. After the acetone extracts was concentrated, the resulting aqueous solution was extracted with EtOAc. The EtOAc layer was dried over anhydrous Na_2SO_4 and concentrated *in vacuo* to yield 2.3 g of solid material. The material was dissolved in a small volume of $CHCl_3$, applied to a silica gel column (30 g, 70–230 mesh, Merck), and eluted stepwise with 100:0, 100:1, 50:1, 10:1, 1:1 and 0:100 (*v*/*v*) of $CHCl_3$–CH_3OH solvents (300 mL each). The $CHCl_3$:CH_3OH=10:1 fraction was concentrated *in vacuo* to dryness to give a brown material (66.0 mg). The material was finally purified by preparative HPLC (column, PEGASIL ODS, 20 mm × 250 mm, Senshu Scientific Co.; solvent, 45% CH_3CN; detection, UV at 210 nm; flow rate, 8.0 mL/min). Under these conditions, hydroxylucilactaene, NG-391, NG393 and lucilactaene were eluted as peaks with retention time of 21, 23, 28 and 38 min. The pooled fractions were concentrated *in vacuo* to dryness to give pure hydroxylucilactaene (1.9 mg), NG-391 (4.0 mg), NG393 (2.3 mg) and lucilactaene (1.8 mg), respectively. The MS and ^1H NMR spectra of these compounds were identical to those reported previously[21–24]. All these samples (1 mg each) were dissolved in 1 mL CH_3OH and used as assay samples.

3-(4,5-Dimethyl-2-thiazolyl)-2,5-diphenyl-2H tetrazolium bromide (MTT) and *p*-nitrophenyl phosphate were purchased from Sigma (St. Louis, MO, USA), Dulbecco's modified Eagle's medium (DMEM), fetal bovine serum (FBS), penicillin/streptomycin, diethnolamine and rhBMP-4 were purchased from Nacalai Tesque (Kyoto, Japan), HyClone (Waltham, MA, USA), Invitrogen (Carlsbad, CA, USA), Wako Pure Chemical Industries (Osaka, Japan) and R&D Systems (Mountain View, CA, USA), respectively.

2.2. *Cell culture*

C2C12 and C2C12 (R206H) cells[20] were cultured in DMEM supplemented with 15% FBS and 100 units/mL penicillin and 100 μg/mL streptomycin (hereafter referred to as medium A) at 37 °C in 5.0% CO_2. Both cells were subcultured once every 3 day.

2.3. *Assay for alkaline phosphatase in BMP-treated C2C12 cells*

Alkaline phosphatase (ALP) activity, a typical marker of osteoblastic differentiation, was measured as described previously[19]. In brief, C2C12 (R206H) cells (7.5×10^3 cells/well) in a 96-well plastic plate were cultured at 37 °C in 5.0% CO_2. Following overnight recovery, the culture media were replaced with 100 μL fresh medium A containing rhBMP-4 (10 ng/mL) and a sample (1 μL in CH_3OH solution). After 48 h incubation, the cells were incubated for 60 min with 100 μL substrate solution (100 mM diethanolamine, 0.5 mM $MgCl_2$ and 1.0 mg/mL *p*-nitrophenylphosphate) at room temperature. The reaction was terminated by adding 50 μL 3 M NaOH, and the absorbance at 405 nm was measured with a Power Wave × 340 (BIO-TEK Instruments, Highland Park, IL, USA).

2.4. *Cytotoxicity*

Cytotoxicity of a compound to C2C12 (R206H) cells was evaluated by the MTT assay[25]. In brief, C2C12 (R206H) cells (7.5×10^3 cells/well) were cultured in 96-well plates in the absence or presence of a compound for 48 h at 37 °C in 5.0% CO_2. After incubation, the cells received 10 μL MTT solution (5.5 mg/mL in phosphate-buffered saline), and were then incubated at 37 °C for 3 h. A 90 μL aliquot of the lysis solution (40% *N,N*-dimethylformamide, 2.0% CH_3COOH, 20% SDS and 0.03 M HCl) was added to each well, and the plates were incubated for 2 h. The absorbance at 550 nm of each well was read with a Power Wave × 340. Inhibition of cell growth is defined as (absorbance-sample/absorbance-control) × 100%. The IC_{50} value is defined as a sample concentration that causes 50% inhibition of cell growth.

2.5. *Reporter gene assay for monitoring BMP signaling*

The effect of a compound on BMP signaling via Smads was examined using a BMP-specific luciferase reporter, Id1WT4F-luc, which is driven by four tandem copies of BRE in the Id1 gene[6]. In brief, C2C12 cells were inoculated at 1.0×10^4 cells/well in 96-well plates with medium A and incubated for 24 h. The cells were transfected with 200 ng of plasmid DNA (40 ng of Id1WT4F-luc, 10 ng of phRL-SV40 and 150 ng of ALK2 (R206H)) using 0.5 μL of Lipofectamine 2000 (Invitrogen) in OPTI-MEM (GIBCO) according to the manufacture's protocol. After 2.5 h incubation, the culture medium was replaced with 100 μL fresh DMEM containing 2.5% FBS without penicillin and streptomycin. After additional 3 h incubation, a compound (1 μL CH_3OH solution) was added to each well and cultured for 24 h. Both firefly and renilla luciferase activities in the cells were determined using Dual Glo Luciferase assay system (Promega, Madison, WI, USA).

3. Results and discussion

In the present study, we screened microbial culture broths for inhibitors of ALP activity of C2C12 (R206H) cells. As a result, structurally related four compounds, lucilactaene[21], hydroxylucilactaene[22], NG-391[23] and NG-393[23,24] (Fig. 1) were isolated from a fungal strain *Fusarium* sp. B88. In fact, all of the compounds inhibited ALP activity in a dose-dependent manner with analogous IC_{50} values of 5.7, 6.8, 6.9 and 6.1 μM (Fig. 2). Although they were originally reported as a cell cycle inhibitor[21],

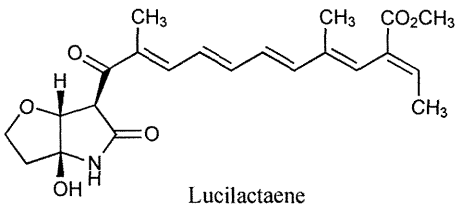

Lucilactaene

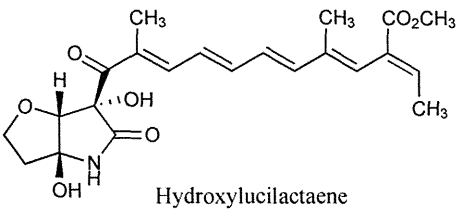

Hydroxylucilactaene

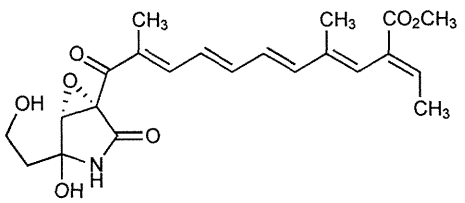

NG-391

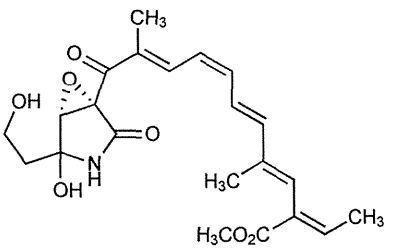

NG-393

Figure 1 Structures of lucilactaene, hydroxylucilactaene, NG-391 and NG-393.

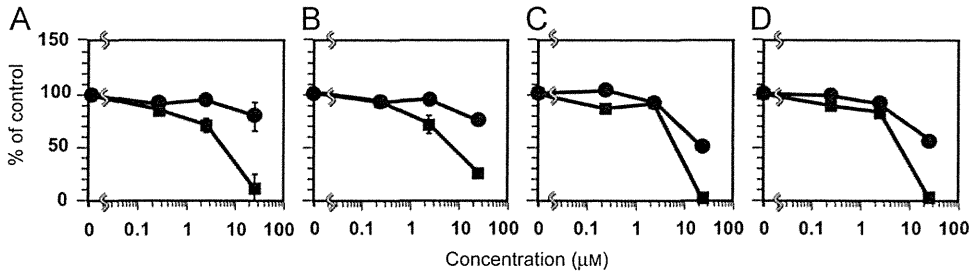

Figure 2 Effect of lucilactaene, hydroxylucilactaene, NG-391 and NG-393 on ALP activity and cytotoxicity of C2C12 (R206H) cells. C2C12 (R206H) cells (7.5×10^3cells/well) were cultured to 70% confluence and then treated with lucilactaene (A), hydroxylucilactaene (B), NG-391 (C) and NG-393 (D) in the presence BMP (10 ng/mL). After 48 h incubation, ALP activity (■) and cytotoxicity (●) were measured as described in Section 2. Values are the mean±SD of three independent experiments.

an anticancer analog[22], promoters of nerve growth factor production[23] and mutagenic agents against the *Salumonella*[24], we first showed that these compounds also inhibit ALP activity, a key marker of osteoblast differentiation of C2C12 (R206H) cells. No marked or very weak cytotoxic effects on C2C12 (R206H) cells were observed at the highest dose (30 μM) of each compound in a MTT assay (Fig. 2).

The ALP activity is one of the markers of osteoblast differentiation *in vitro* and *in vivo*. The induction of ALP activity in C2C12 cells is an output through the multiple intracellular events initiated by the activation of BMP receptors. To examine direct effect of those compounds on BMP signaling, we determined Id1WT4F-luc activity in C2C12 cells. The luciferase activity in Id1WT4F-luc is driven by BRE in the Id1 gene, which is recognized by a complex of phosphorylated Smad1/5/8 and Smad4. Since Smad1/5/8 is phosphorylated by BMP type I receptors including ALK2, the formation of Smad complexes on BRE and the induction of reporter activity is highly specific for BMP signal transduction. As shown in Fig. 3, NG-391 and NG-393 inhibited luciferase activity of Id1WT4F-luc in C2C12 cells with IC_{50} values of 1.4 and 2.1 μM, respectively. These concentrations were much lower than those of cytotoxic effects. Lucilactaene and hydroxylucilactaene showed no effect on luciferase activity at 2.5 μM (Fig. 3), and inhibited the activity at 20 μM probably due to cytotoxic effects.

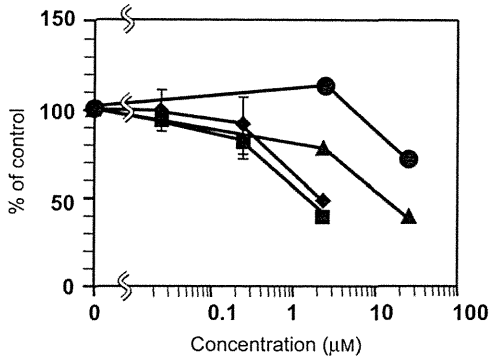

Figure 3 Effect of lucilactaene, hydroxylucilactaene, NG-391 and NG-393 on BMP signaling in C2C12 (Id1-BRE) cells. C2C12 cells (1.0×10^4 cells/well) were cultured for 24 h and then Id1-WT4F-luc, phRL-SV40 and ALK2 (R206H) were co-transfected to construct C2C12 (Id1-BRE) cells. After 2.5 h incubation, the culture media were replaced with DEME containing 2.5% FBS without penicillin and streptomycin. After another 3 h incubation, the cells were treated with lucilactaene (●), hydroxylucilactaene (▲), NG-391 (■) and NG-393 (♦). Luciferase activities in the cell extracts were determined using the Dual Glo Luciferase assay system as described in Section 2. Values are the mean±SD of three independent experiments.

Our findings suggest that NG-391 and NG-393 may inhibit an early event(s) in BMP signal transduction because they inhibited the BMP-specific luciferase reporter activity, which expression is directly regulated by Smads. On the other hand, lucilactaene and hydroxylucilactaene may inhibit a different event(s) from that NG compounds. To the best of our knowledge, this is the first report of BMP signal inhibitors of natural origin. BMP activity is controlled at multiple steps in signal transduction. It was reported that BMP antagonists such as noggin and follistatin inhibit a binding step of BMPs to the receptors in the extracellular space[26,27] and that an intracellular domain-truncated type I receptor, BAMBI, inhibits BMP signaling by acting as a dominant negative receptor on the cell membrane[28]. In contrast, several types of BMP inhibitors act in the intracellular spaces; FKBP-12 and I-Smads, such as Smad6 and Smad7, bind to the GS domain and kinase domain of the type I receptors, respectively, and block the kinase activity[29]. The chemical BMP inhibitors, dorsomorphin[13,14] and LDN-193189[15], have been shown to bind to the ATP-binding pocket of the type I receptors to prevent phosphorylation of Smads[30]. Two types of protein phosphatases, protein phosphatase Mg^{2+}-dependent 1A and small C-terminal protein phosphatases, inhibits Smads and further downstream effectors in BMP signaling[31]. Since NG-391 and NG-393 inhibited BMP-induced ALP activity and the luciferase reporter activity, these compounds may target a step(s) between BMP binding to the receptor and activation of Smads on the BRE. Further studies will be needed to elucidate molecular mechanisms of the inhibition of BMP signaling by the compounds found in this study. We expect that these compounds will provide a new direction in the development of FOP therapeutics.

Acknowledgments

We wish to thank Dr. K. Nagai and Ms. N. Sato (Kitasato University) for measurements of mass spectra and NMR, respectively.

References

1. Paget S. The distribution of secondary growths in cancer of the breast. 1889. *Cancer Metastasis Rev* 1989;**8**:98-101.
2. Urist MR, Wallace TH, Adams T. The function of fibrocartilaginous fracture callus. observations on transplants labeled with tritiated thymidine. *J Bone Joint Surg Br* 1965;**47**:304–18.
3. Gazzerro E, Canalis E. Bone morphogenetic proteins and their antagonists. *Rev Endocr Metab Disord* 2006;**7**:51–65.
4. Shi Y, Massagué J. Mechanisms of TGF-beta signaling from cell membrane to the nucleus. *Cell* 2003;**113**:685–700.
5. Macías-Silva M, Hoodless PA, Tang SJ, Buchwald M, Wrana JL. Specific activation of Smad1 signaling pathways by the BMP7 type I receptor, ALK2. *J Biol Chem* 1998;**273**:25628–36.
6. Katagiri T, Imada M, Yanai T, Suda T, Takahashi N, Kamijo R. Identification of a BMP-responsive element in Id1, the gene for inhibition of myogenesis. *Genes Cells* 2002;**7**:949–60.
7. Peltier L.F. A case of extraordinary exostoses on the back of a boy. 1740. John Freke (1688–1756). *Clin Orthop Relat Res* 1998; **346**:5–6.
8. Glaser DL, Economides AN, Wang L, Liu X, Kimble RD, Fandl JP, et al. *In vivo* somatic cell gene transfer of an engineered Noggin mutein prevents BMP4-induced heterotopic ossification. *J Bone Joint Surg Am* 2003;**85**:2332–42.
9. Kaplan FS, McCluskey W, Hahn G, Tabas JA, Muenke M, Zasloff MA. Genetic transmission of fibrodysplasia ossificans progressiva. Report of a family. *J Bone Joint Surg Am* 1993; **75**:1214–20.
10. Kaplan FS, Zasloff MA, Kitterman JA, Shore EM, Hong CC, Rocke DM. Early mortality and cardiorespiratory failure in patients with fibrodysplasia ossificans progressiva. *J Bone Joint Surg Am* 2010;**92**:686–91.
11. Connor JM, Evans DA. Fibrodysplasia ossificans progressiva. The clinical features and natural history of 34 patients. *J Bone Joint Surg Br* 1982;**64**:76–83.
12. Shore EM, Xu M, Feldmn GJ, Fenstermacher DA, Cho TJ, Choi IH, et al. A recurrent mutation in the BMP type I receptor ACVR1 causes inherited and sporadic fibrodysplasia ossificans progressiva. *Nat Genet* 2006;**38**:525–7.
13. Yu PB, Hong CC, Sachidanandan C, Babitt JL, Deng DY, Hoyng SA, et al. Dorsomorphin inhibits BMP signals required for embryogenesis and iron metabolism. *Nat Chem Biol* 2008;**4**:33–41.
14. Hao J, Ho JN, Lewis JA, Karim KA, Daniels RN, Gentry PR, et al. *In vivo* structure-activity relationship study of dorsomorphin analogues identifies selective VEGF and BMP inhibitors. *ACS Chem Biol* 2010;**5**:245–53.
15. Cuny GD, Yu PB, Laha JK, Xing X, Liu JF, Lai CS, et al. Structure-activity relationship study of bone morphogenetic protein (BMP) signaling inhibitors. *Bioorg Med Chem Lett* 2008;**18**:4388–92.
16. Yu PB, Deng DY, Lai CS, Hong CC, Cuny GD, Bouxsein ML, et al. BMP type I receptor inhibition reduces heterotopic [corrected] ossification. *Nat Med* 2008;**14**:1363–9.
17. Katagiri T, Yamaguchi A, Komaki M, Abe E, Takahashi N, Ikeda T, et al. Bone morphogenetic protein-2 converts the differentiation pathway of C2C12 myoblasts into the osteoblast lineage. *J Cell Biol* 1994;**127**:1755–66.
18. Fukuda T, Kanomata K, Nojima J, Kokabu S, Akita M, Ikebuchi K, et al. A unique mutation of ALK2, G356D, found in a patient with fibrodysplasia ossificans progressiva is a moderately activated BMP type I receptor. *Biochem Biophys Res Commun* 2008;**377**: 905–9.
19. Ohte S, Shin M, Sasanuma H, Yoneyama K, Akita M, Ikebuchi K, et al. A novel mutation of ALK2, L196P, found in the most benign case of fibrodysplasia ossificans progressiva activates BMP-specific intracellular signaling equivalent to a typical mutation, R206H. *Biochem Biophys Res Commun* 2011;**407**:213–8.
20. Fukuda T, Kohda M, Kanomata K, Nojima J, Nakamura A, Kamizono J, et al. Constitutively activated ALK2 and increased SMAD1/5 cooperatively induce bone morphogenetic protein signaling in fibrodysplasia ossificans progressiva. *J Biol Chem* 2009;**284**:7149–56.
21. Kakeya H, Kageyama S, Nie L, Onose R, Okada G, Beppu T, et al. Lucilactaene, a new cell cycle inhibitor in p53-transfected cancer cells, produced by a Fusarium sp. *J Antibiot* 2001;**54**:850–4.
22. Bashyal BP, Faeth SH, Gunatilaka AA. 13a-Hydroxylucilactaene and other metabolites of an endophytic strain of *Fusarium acuminatum*. *Nat Prod Commun* 2007;**2**:547–50.
23. Bashyal BP, Gunatilaka AA. Tricinonoic acid and tricindiol, two new irregular sesquiterpenes from an endophytic strain of *Fusarium tricinctum*. *Nat Prod Res* 2010;**24**:349–56.
24. Krasnoff SB, Sommers CH, Moon YS, Donzelli BG, Vandenberg JD, Churchill AC, et al. Production of mutagenic metabolites by *Metarhizium anisopliae*. *J Agric Food Chem* 2006;**54**:7083–8.
25. Mosmann J. Rapid colorimetric assay for cellular growth and survival: application to proliferation and cytotoxicity assays. *Immunol Methods* 1983;**65**:55–63.
26. Secondini C, Wetterwald A, Schwaninger R, Thalmann GN, Cecchini MG. The role of the BMP signaling antagonist noggin in the development of prostate cancer osteolytic bone metastasis. *PLoS One* 2011;**6**:e16078.
27. Pierre A, Pisselet C, Monget P, Monniaux D, Fabre S. Testing the antagonistic effect of follistatin on BMP family members in ovine granulosa cells. *Reprod Nutr Dev* 2005;**45**:419–25.
28. Paulsen M, Legewie S, Eils R, Karaulanov E, Niehrs C. Negative feedback in the bone morphogenetic protein 4 (BMP4) synexpression group governs its dynamic signaling range and canalizes development. *Proc Natl Acad Sci USA* 2011;**108**:10202–7.
29. Yamaguchi T, Kurisaki A, Yamakawa N, Minakuchi K, Sugino H. FKBP12 functions as an adaptor of the Smad7-Smurf1 complex on activin type I receptor. *J Mol Endocrinol* 2006;**36**: 569–79.
30. Boergermann JH, Kopf J, Yu PB, Knaus P. Dorsomorphin and LDN-193189 inhibit BMP-mediated Smad, p38 and Akt signalling in C2C12 cells. *Int J Biochem Cell Biol* 2010;**42**:1802–7.
31. Kokabu S, Ohte S, Sasanuma H, Shin M, Yoneyama K, Murata E, et al. Suppression of BMP-Smad signaling axis-induced osteoblastic differentiation by small C-terminal domain phosphatase 1, a Smad phosphatase. *Mol Endocrinol* 2011;**25**:474–81.

International Scholarly Research Network
ISRN Orthopedics
Volume 2012, Article ID 396718, 5 pages
doi:10.5402/2012/396718

Research Article

The Biomechanical Effect of the Sensomotor Insole on a Pediatric Intoeing Gait

Akiyoshi Mabuchi,[1] Hiroshi Kitoh,[1] Masato Inoue,[2] Mitsuhiko Hayashi,[3] Naoki Ishiguro,[1] and Nobuharu Suzuki[4]

[1] *Department of Orthopaedic Surgery, Nagoya University Graduate School of Medicine, 65 Tsurumai, Showa-ku, Nagoya, Aichi 466-8550, Japan*
[2] *Department of Electrical Engineering and Bioscience, School of Advanced Science and Engineering, Waseda University, 3-4-1 Okubo, Shinjyuku-ku, Tokyo 169-8555, Japan*
[3] *Semui College, Tokai College of Medical Science, 2-7-2 Meiekiminami, Nakamura-ku, Nagoya, Aichi 450-0003, Japan*
[4] *The Institute for Developmental Research, Aichi Human Service Center, 713-8 Kagiya-cho, Kasugai, Aichi 480-0392, Japan*

Correspondence should be addressed to Hiroshi Kitoh, hkitoh@med.nagoya-u.ac.jp

Received 29 July 2012; Accepted 1 October 2012

Academic Editors: C.-H. Lee, A. Leithner, and S.-J. Lim

Background. The sensomotor insole (SMI) has clinically been shown to be successful in treating an intoeing gait. We investigated the biomechanical effect of SMI on a pediatric intoeing gait by using three-dimensional gait analysis. *Methods.* Six patients with congenital clubfeet and four patients with idiopathic intoeing gait were included. There were five boys and five girls with the average age at testing of 5.6 years. The torsional profile of the lower limb was assessed clinically. Three-dimensional gait analysis was performed in the same shoes with and without SMI. *Results.* All clubfeet patients exhibited metatarsal adductus, while excessive femoral anteversion and/or internal tibial torsion was found in patients with idiopathic intoeing gait. SMI showed significant decreased internal rotation of the proximal femur in terminal swing phase and loading response phase. The internal rotation of the tibia was significantly smaller in mid stance phase and terminal stance phase by SMI. In addition, SMI significantly increased the walking speed and the step length. *Conclusions.* SMI improved abnormal gait patterns of pediatric intoeing gait by decreasing femoral internal rotation through the end of the swing phase and the beginning of the stance phase and by decreasing tibial internal rotation during the stance phase.

1. Introduction

Gait disorders have become the most prevalent orthopedic problems in children. One of the most common complaints of the gait disorders in infants and children is an intoeing gait, which is caused by excessive anteversion of the proximal femur, internal tibial torsion, and/or metatarsal adductus [1–5]. A careful evaluation of the children is essential to rule out serious pathological conditions such as cerebral palsy, infantile Blount's disease, metabolic bone diseases, and skeletal dysplasias. An intoeing gait in the majority of patients without these pathological conditions is a minor problem and is observed to spontaneously improve with time [2]. The condition, however, sometimes produces functional problems such as frequent tripping. The parents or grandparents are concerned that the child will have a permanent disability or that the condition will interfere with the child's physical performance; thus they sometimes hope for some treatments [5]. A shoe modification with wedges or arch supports is one of the tolerable nonsurgical treatments for children to correct an intoeing gait and modify the gait pattern.

The sensomotor insole (SMI), which had been introduced by the German shoemaker Jarhling, was originally developed to improve abnormal gait patterns in children with spastic gait [6, 7]. It was expected to change the muscle tone of the lower limbs by stimulating the proprioceptors of the sole. Jahrling and Rockenfeller demonstrated improvement of the gait patterns in cerebral palsy patients with flexible equinus or equinovarus deformities using SMI [6]. This information prompted us to try the use of SMI for

Table 1: Summary of the patients.

Patients	Age (years)	Sex	Laterality	Diagnosis	Deformities
1	3	F	Bilateral	Clubfoot	Metatarsal adductus
2	7	M	Bilateral	Clubfoot	Metatarsal adductus
3	9	M	Bilateral	Clubfoot	Metatarsal adductus
4	5	F	Bilateral	Idiopathic intoeing gait	Excessive femoral anteversion
5	6	M	Bilateral	Clubfoot	Metatarsal adductus
6	7	F	Bilateral	Idiopathic intoeing gait	Excessive femoral anteversion and increased tibial internal torsion
7	3	M	Right side	Clubfoot	Metatarsal adductus
8	7	F	Bilateral	Idiopathic intoeing gait	Increased tibial internal torsion
9	4	F	Bilateral	Idiopathic intoeing gait	Excessive femoral anteversion
10	5	M	Left side	Clubfoot	Metatarsal adductus

* F: female, M: male.

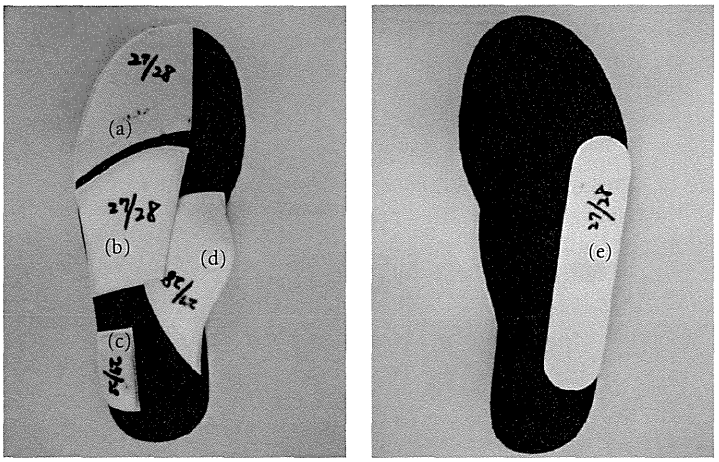

(A) (B)

Figure 1: The upper (A) and the reverse (B) views of the sensomotor insole used for this study. It is consisted of five bars including a toe bar (a), a retro bar (b), a lateral heel bar (c), a medial heel bar (d), and a last bar (e).

a pediatric intoeing gait, since the patients usually have more flexible feet than the cerebral palsy patients. In the present study, the effects of SMI on a pediatric intoeing gait were evaluated using the three-dimensional (3D) gait analysis with a Vicon motion capture system.

2. Materials and Methods

The parents of patients treated with SMI for their intoeing gait at our institution between January 2009 and December 2010 were invited to have their child participate in this prospective study, which was approved by an institutional review board. Patients who had rigid deformities of the feet with an ankle range of motion less than 30 degrees or forefoot abduction less than 10 degrees were excluded from this study. Patients who underwent gait analysis with the use of other systems were also excluded. Some patients could not complete testing because of the child's uncooperative behavior. Overall, 10 patients were included in this series (Table 1). There were five boys and five girls, and the average age at testing was 5.6 years (range, 3–9 years). Bilateral intoeing gait was observed in eight, right side in one, and left side in one. Among six congenital clubfeet patients who had initially been treated with serial casting and braces, two patients were additionally treated with extensive soft tissue releases. There were four patients in an idiopathic intoeing gait. The torsional profile was assessed with the patient prone on the examining table, as described by Staheli et al., so that the examiner can determine the amount of internal and external rotation of the hip as an indication of the amount of femoral anteversion, measure the thigh-foot angle in order to estimate tibial torsion, and examine the shape of the lateral border of the foot to assess the presence of metatarsal adductus [2].

SMI comprises of five exclusive bars, including medial and lateral heel bars, a retro bar, a toe bar, and a lateral wedge (Figure 1). Before first application of the insole, patients were individually ground to size Velcro trial elements that were attached to a base sole by the orthopaedic shoe technician. The trial elements can be readjusted

repeatedly until the desired gait pattern has been achieved. Once the final position of the bars has been determined, the individual SMI was made up in the workshop using the care set [8].

The computerized motion analysis tests were performed with a six-camera VICON 3D motion system (Vicon MX system, Oxford, UK) during walking at a self-selected speed along a five-meter walkway using 16 passive retroreflective markers attached to specific bony landmarks of the lower extremities and the pelvis. Patients underwent gait analysis in the same shoes with and without SMI. Walking speed, stride length, and cadences were calculated using the Vicon Plug-in Gait (Vicon MX system, Oxford, UK), and the 3D joint kinematic data were obtained at 100 Hz for the hips, knees and ankles in the sagittal plane and the hips and knees in the coronal and transverse planes from bilateral lower extremities. Comparisons in walking speed, step length, cadences, and joint kinematic data of the lower extremities were made between the conditions with and without SMI. The data were analyzed using the VICON NEXUS Plug-in Gait and the custom-made software; the VICON Normalizer ver. 1.54. Gait cycle events that were defined by Perry were adopted for descriptions in this study [9].

Paired t-test was conducted to determine any difference among the demographics of the two groups (with and without SMI). The level of significance was set at $P < 0.05$. Analysis was performed with SPSS version 16.0 (SPSS Inc, Chicago, IL, USA).

3. Results

All patients with clubfeet showed residual metatarsal adductus without apparent hindfoot deformities. In four patients with idiopathic intoeing gait, excessive anteversion of the proximal femur was seen in three, and internal tibial torsion was found in two (one of the four patients had both deformities) (Table 1). Improvement of the gait pattern was clinically recognized after a couple of steps on wearing SMI in most patients.

There were significant differences in transverse plane motions of the hip and knee joints between the patients with and without SMI. SMI decreased internal rotation of the proximal femur relative to the pelvis in loading response phase ($-18.3° \pm 28.1°$ versus $-21.6° \pm 28.0°$, $P = 0.009$) and terminal swing phase ($-16.3° \pm 27.4°$ versus $-19.0° \pm 26.4°$, $P = 0.047$) (Table 2, Figure 2). SMI also decreased internal rotation of the tibia relative to the femur in mid stance phase ($0.7° \pm 12.5°$ versus $-2.0° \pm 14.9°$, $P = 0.030$) and terminal stance phase ($1.4° \pm 11.9°$ versus $-2.3° \pm 14.5°$, $P = 0.042$) (Table 3, Figure 3). There were no significant differences of the hip and knee kinematics in the sagittal plane between the patients with and without SMI. Ankle dorsiflexion was increased in loading response phase and terminal swing phase and decreased in terminal stance phase and terminal swing phase on wearing SMI. In regard to cadence parameters, SMI significantly increased the walking speed (67.9 m/min versus 64.9 m/min, $P < 0.001$) and the stride length (500 mm versus 477 mm, $P < 0.001$), although cadence did not differ between the two groups (137.6 steps/min versus 136.7 steps/min, $P = 0.89$) (Table 4).

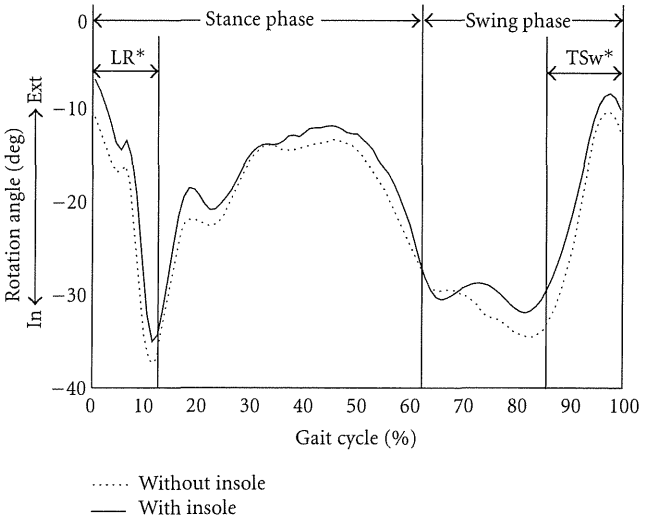

FIGURE 2: Average femoral rotation in transverse plane for patients with the sensomotor insole (solid) and without the insole (dotted). Positive values represent external rotation and negative values represent internal rotation. The patients with the sensomotor insole group demonstrated an increased external rotation of the proximal femur relative to the pelvis from the end of the swing phase to the beginning of the stance phase. LR: loading response, TSw: terminal swing, In: internal rotation, Ext: external rotation, *statistically significant.

TABLE 2: Femoral rotation in transverse plane.

Gait cycle	With the SMI ($n = 18$)	Without the SMI ($n = 18$)	P value
Loading response	$-18.3° \pm 28.1°$	$-21.6° \pm 28.0°$	0.009*
Mid stance	$-20.5° \pm 30.0°$	$-22.5° \pm 31.0°$	0.076
Terminal stance	$-12.4° \pm 28.0°$	$-13.6° \pm 30.7°$	0.275
Preswing	$-17.7° \pm 28.9°$	$-19.8° \pm 30.0°$	0.051
Initial swing	$-29.0° \pm 27.7°$	$-29.8° \pm 30.0°$	0.635
Mid swing	$-30.3° \pm 26.8°$	$-33.4° \pm 26.9°$	0.059
Terminal swing	$-16.3° \pm 27.4°$	$-19.0° \pm 26.4°$	0.047*

SMI: sensomotor insole.
*Statistically significant.
±: External rotation/internal rotation.

4. Discussion

Li and Leong emphasized the importance of a correct diagnosis and understanding the causes and natural course of the condition in the management of a pediatric intoeing gait [10]. Thackeray and Beeson pointed out that identification of the level of torsional deformities (excessive femoral anteversion, internal tibial torsion, or metatarsal adductus) that produced an intoeing gait should be essential for planning of the specific intervention [3]. The present study, however, demonstrated that SMI improved abnormal gait patterns not only children with idiopathic intoeing gait but also those

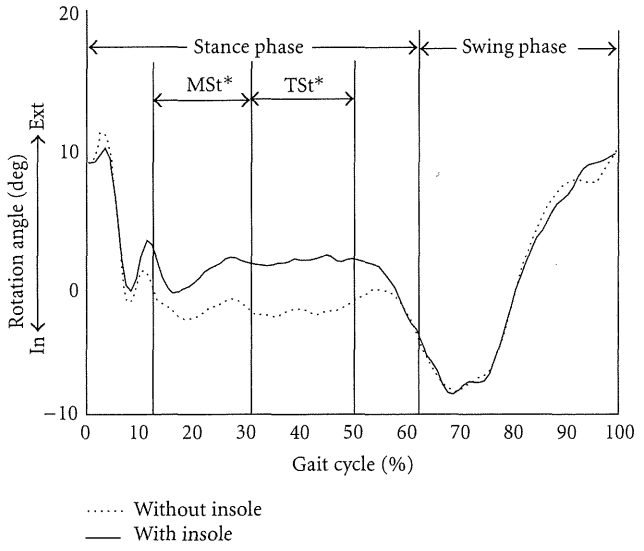

FIGURE 3: Average tibial rotation in transverse plane for the patients with the sensomotor insole (solid) and without the insole (dotted). Positive values represent external rotation and negative values represent internal rotation. The patients with the sensomotor insole group demonstrated an increased external rotation of the tibia relative to the femur in the middle of stance phase. MSt: mid stance, TSt: terminal stance, In: internal rotation, Ext: external rotation, *statistically significant.

TABLE 3: Tibial rotation in transverse plane.

Gait cycle	With the SMI (n = 18)	Without the SMI (n = 18)	P value
Loading response	4.6° ± 15.9°	4.2° ± 16.0°	0.767
Mid stance	0.7° ± 12.5°	−2.0° ± 14.9°	0.030*
Terminal stance	1.4° ± 11.9°	−2.3° ± 14.5°	0.042*
Preswing	−0.2° ± 10.7°	−1.6° ± 12.8°	0.317
Initial swing	−7.0° ± 14.0°	−7.0° ± 15.7°	0.882
Mid swing	−1.2° ± 15.8°	−0.8° ± 17.4°	0.752
Terminal swing	7.4° ± 13.6°	7.4° ± 14.7°	0.909

SMI: sensomotor insole.
*Statistically significant.
±: External rotation/internal rotation.

TABLE 4: Gait parameter.

	With the SMI (n = 18)	Without the SMI (n = 18)	P value
Walking speed (m/min)	67.9 ± 9.4	64.9 ± 11.5	<0.001*
Step length (mm)	500 ± 81	477 ± 85	<0.001*
Cadence (steps/min)	137.6 ± 16.0	136.7 ± 14.9	0.89

SMI: sensomotor insole
*Statistically significant.

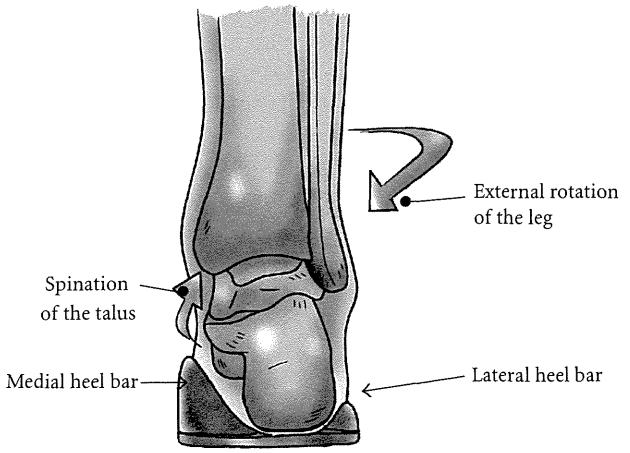

FIGURE 4: Hypothetical role of the medial and the lateral heel bar (rear view). The calcaneous kept in neutral position between the medial and the lateral heel bar suppresses pronation of the subtalar joint, leading to reduction of the internal rotation of the leg.

with congenital clubfeet, who had deformities of different levels in lower limbs. Although SMI cannot correct dynamic and structural abnormalities of the lower extremities of feet and its long-term effectiveness is unknown, it is one of the easy and effective treatment options in the management of a pediatric intoeing gait.

SMI inhibited internal rotation of the leg in loading response phase, which is usually observed in normal gait [11]. Nakajima reported that the foot progression angle, which is the angle formed by the direction of gait progression and the foot axis at mid stance, was reduced by using a lateral wedged sole, but it recovered in the use of a lateral wedge and an arch support that resembles SMI [12]. The present study revealed that the decreased internal rotation of the lower limb by SMI was shown to be due to decreased internal rotation of the proximal femur through the end of the swing phase and the beginning of the stance phase and decreased internal rotation of the tibia during the mid and terminal stance phases. Although the precise biomechanical effect of this specific insole on the hip and knee joints remains unknown, it is recognized that the leg-ankle-foot alignment is affected by the varus-valgus of the calcaneus [11]. We speculated that the calcaneus stabilized in neutral position between the medial and the lateral heel bar at the initial contact may provide favorable effects on entire lower limbs by suppressing pronation of the subtalar joint which is accompanied by internal rotation of the leg (Figure 4).

In addition to changing the rotational profile of the lower limb, SMI accelerated children's walking speed and increased stride lengths. The increase of the walking speed depended on the increase of the stride length because cadence did not show significant differences between children with and without SMI. SMI increased external rotation of the femur relative to the pelvis during the end of the swing phase, which reflected the internal rotation of the pelvis relative to the femur. The increment of stride lengths could be due to internally rotated pelvis toward the direction of progression in walking [13].

There are several limitations to this study. Young children were tested under a nonthreatening environment with parents present and distractions such as toys available in

the present study, but the likelihood of not walking in their normal fashion while undergoing instrumented gait analysis is questionable. The foot progression angle, which is the most important variable to be measured, was not addressed in the present study because we unfortunately did not possess a force plate instrument that is indispensable to show the accurate direction of gait progression. The measurements of children without SMI may not reflect the actual gait situation because the shoes, which were adjusted on wearing SMI, would be a little large when children put them on without SMI. Finally, the number of patients examined in this study was limited because of difficulties in performing the gait analysis for toddlers or naughty children.

In conclusion, SMI improved an intoeing gait pattern in patients with congenital clubfeet and idiopathic intoeing by externally rotating the proximal femur through the end of the swing phase and the beginning of the stance phases and externally rotating the tibia during the mid and terminal stance phase, resulting in acceleration of the walking speed and increase in the stride lengths.

Conflict of Interests

The authors declare that they have no conflict of interests.

References

[1] M. O. Tachdjian, *Pediatric Orthopaedics*, chapter 5, 4th edition, 2008.

[2] L. T. Staheli, M. Corbett, C. Wyss, and H. King, "Lower-extremity rotational problems in children. Normal values to guide management," *Journal of Bone and Joint Surgery*, vol. 67, no. 1, pp. 39–47, 1985.

[3] C. Thackeray and P. Beeson, "In-toeing gait in children. A review of the literature," *Foot*, vol. 6, no. 1, pp. 1–4, 1996.

[4] M. Jacquemier, Y. Glard, V. Pomero, E. Viehweger, J. L. Jouve, and G. Bollini, "Rotational profile of the lower limb in 1319 healthy children," *Gait and Posture*, vol. 28, no. 2, pp. 187–193, 2008.

[5] J. P. Blackmur and A. W. Murray, "Do children who in-toe need to be referred to an orthopaedic clinic?" *Journal of Pediatric Orthopaedics Part B*, vol. 19, no. 5, pp. 415–417, 2010.

[6] L. Jahrling and B. Rockenfeller, "Sensomotor insole fabrication: action and reaction," *Orthopädie Schuhtechnik Magazine*, vol. 9, pp. 50–55, 2006 (German).

[7] K. H. Schott, "The concept of sensomotor insole by Lother Jahrling," *Orthopädie Schuhtechnik Magazine*, vol. 6, pp. 36–43, 2003 (German).

[8] L. Jahrling, "Result of sports and sensomotor insole," *Orthopädieschuhtechnik*, vol. 7, no. 8, pp. 35–36, 2004.

[9] J. Perry, *Gait Analysis: Normal and Pathological Function*, chapter 2, 1992.

[10] Y. H. Li and J. C. Y. Leong, "Intoeing gait in children," *Hong Kong Medical Journal*, vol. 5, no. 4, pp. 360–366, 1999.

[11] P. K. Levangie and C. C. Norkin, *Joint Structure and Function: A Comprehensive Analysis*, chapter 12, 4th edition, 2005.

[12] K. Nakajima, W. Kakihana, T. Nakagawa et al., "Addition of an arch support improves the biomechanical effect of a laterally wedged insole," *Gait and Posture*, vol. 29, no. 2, pp. 208–213, 2009.

[13] J. Perry, *Gait Analysis: Normal and Pathological Function*, chapter 3, 1992.

Eur Spine J (2013) 22:205–210
DOI 10.1007/s00586-012-2573-8

ORIGINAL ARTICLE

Interobserver and intraobserver reliability of the classification and diagnosis for ossification of the posterior longitudinal ligament of the cervical spine

Hitoshi Kudo · Toru Yokoyama · Eiki Tsushima · Atsushi Ono · Takuya Numasawa · Kanichiro Wada · Sunao Tanaka · Satoshi Toh

Received: 9 March 2011 / Revised: 1 December 2011 / Accepted: 3 November 2012 / Published online: 21 November 2012

Abstract
Purpose Ossification of the posterior longitudinal ligament (OPLL) of the cervical spine has been classified into four types by lateral plain radiographs, but the reliability of the classification and of the diagnosis of either cervical OPLL or cervical spondylotic myelopathy (CSM) was unknown. We investigated the interobserver and intraobserver reliability of the classification and diagnosis for OPLL by radiographs and computed tomography (CT) images.
Methods A total of 16 observers classified each patient's images into five groups; OPLL continuous, segmental, mixed, circumscribed type, or CSM. To evaluate interobserver reliability, the observers first classified only radiograph images, and next both radiographs and CT images. On another day they followed the same procedure to evaluate intraobserver reliability. We also evaluated interobserver and intraobserver reliability of the diagnosis of either cervical OPLL or CSM.
Results Interobserver reliability of the classification with radiographs only showed moderate agreement, but interobserver reliability with both radiographs and CT images showed substantial agreement. Intraobserver of reliability the classification was also improved by additional CT images. Interobserver reliability of the diagnosis with both radiographs and CT images was almost similar to with radiographs only. Intraobserver reliability of the diagnosis was improved by additional CT images.
Conclusions This study suggested that the reliability of the classification and diagnosis for cervical OPLL was improved by additional CT images. We propose that diagnostic criteria for OPLL include both radiographs and CT images.

Keywords Interobserver and intraobserver reliability · Ossification of the posterior longitudinal ligament (OPLL) · Cervical spondylotic myelopathy (CSM) · Radiograph · Computed tomography (CT) image

Introduction

Ossification of the posterior longitudinal ligament (OPLL) of the spine is characterized by ectopic bone formation in the spinal ligaments. In 1960, Tsukimoto [1] first reported OPLL in Japan and OPLL is a common disorder among Japanese and other Asian populations. The incidence of OPLL in Japan is about 3 % (1.8–4.1 %) [2], and the male/female ratio for patients diagnosed as having OPLL is 1.96 (1.1–3.0) [3]. OPLL causes compression of the spinal cord and leads to various degrees of myelopathy. Typical symptoms of OPLL are sensory and motor disturbance of the upper and lower extremities, abnormal reflexes, hyperresponsive deep reflexes, and bladder-bowel dysfunction. Various degrees of dysfunction, such as precise action and gait disturbance, lead to the restriction of activities involved in daily living and the deterioration of quality of life.

H. Kudo · A. Ono · T. Numasawa · K. Wada · S. Tanaka · S. Toh
Department of Orthopaedic Surgery,
Hirosaki University Graduate School of Medicine,
5 Zaifu-cho, Hirosaki 036-8562, Japan

T. Yokoyama (✉)
Department of Orthopaedic Surgery, Odate Municipal General Hospital, 3-1 Yutaka-cho, Odate 017-0885, Japan
e-mail: yokoyama@odate-hp.odate.akita.jp

E. Tsushima
Hirosaki University Graduate School of Health Sciences,
66-1 Hon-cho, Hirosaki 036-8564, Japan

The occurrence and development of OPLL involve many environmental, systemic, and local factors. Examples of factors are diet, metabolic or endocrinological background, and mechanical stress [4]. Genetic susceptibilities to OPLL have been identified by several groups. COL11A2 [5], NPPS [6], and COL6A1 [7] have been reported as candidate genes for OPLL.

According to the report of the Investigation Committee on OPLL of the Japanese Ministry of Public Health and Welfare (now the Japanese Ministry of Health, Labour, and Welfare), OPLL of the cervical spine has been classified into four types by lateral plain radiographs [8, 9]: (1) continuous; a long lesion extending over several vertebral bodies, (2) segmental; one or several separate lesions behind the vertebral bodies, (3) mixed; a combination of the continuous and segmental types, and (4) circumscribed; mainly located posterior to a disc space (Fig. 1).

The guidelines committee of the Japan Orthopaedic Association proposed that the clinical diagnostic criteria for OPLL need the radiograph findings as well as the clinical symptoms (Table 1) [10]. A small ossification area that is not visible on radiographs but can be detected only by computed tomography (CT) images does not fulfill the diagnostic definition for OPLL. Therefore, it is sometimes difficult to differentiate OPLL from cervical spondylotic myelopathy (CSM) only by radiographs. Recently, sagittal CT images are used for diagnosis of OPLL, and we can evaluate the ossification area in detail with CT images. But CT images are not included in the clinical guidelines for OPLL. (As a proposal, the use of CT images is advised.) Accurate classification and diagnosis for cervical OPLL is important for treatment and prognosis, but the reliability of the classification has not been evaluated.

The purpose of this study was to investigate the interobserver and intraobserver reliability of the classification and diagnosis for cervical OPLL by radiographs and CT images.

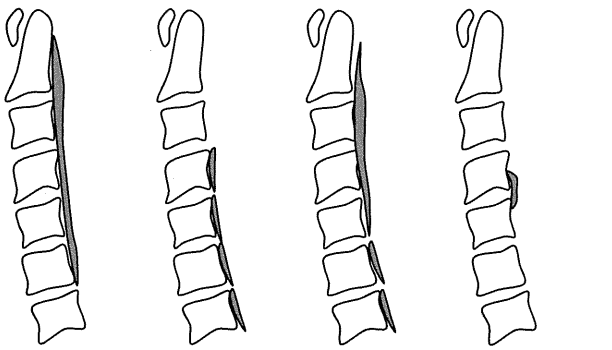

Fig. 1 The classification for cervical OPLL

Table 1 Diagnostic criteria for cervical OPLL

(1) Image requirement: OPLL is visible on lateral plain radiograph. If lower cervical OPLL is not visible adequately, tomography or CT image is advised. Small ossification area that is visible on only CT image is not included in OPLL
(2) Clinical requirement: The patients have the following clinical symptom:
(a) Symptoms of compressive cervical spinal cord involvement
(b) Symptoms of nerve root
(c) Disorder of cervical spinal movement

Materials and methods

Observers

Because experience in clinical practice was expected to affect the reliability of the classification and diagnosis, the observers were separated into two groups by their level of experience in orthopaedic surgery. One group included eight spine surgery specialists, and the other included eight residents in the orthopaedic residency programs. A total of 16 observers classified each patient's image into five groups: continuous, segmental, mixed, circumscribed type OPLL, or CSM.

Patients and images

Fifty-seven patients (41 males and 16 females) with a diagnosis of OPLL or CSM were included in this study. The films of radiographs and CT images were scanned by computer (radiographs; 200 dpi, CT images; 300 dpi), and each image was displayed on a computer screen. The magnification of the images depended on each observer. To differentiate the ossification area clearly, we did not use CT myelography.

Evaluation for reliability

To evaluate interobserver reliability, the observers classified images only by radiographs, and next they classified by both radiographs and CT images. To evaluate intraobserver reliability, the observers followed the same procedure on another day (more than 24 h later). We used not only radiographs but also CT images to evaluate the degree of improvement of reliability, and we also evaluated difference in reliabilities between only radiographs and both radiographs and CT images. The reliability was examined with Cohen's kappa values. Interpretation of the strength of agreement determined with the kappa values was given by adopting the criteria of Landis and Koch [11]: >0.81; Almost perfect, 0.61–0.80; Substantial, 0.41–0.60; Moderate, 0.21–0.40; Fair, 0–0.20; Slight.